RADIATION EFFECTS IN QUARTZ RESONATORS

By

STEPHEN PAUL DOHERTY

Bachelor of Arts
University of Dublin
Trinity College
1975

Master of Science
University of Dublin
Trinity College
1978

Submitted to the Faculty of the
Graduate College of the
Oklahoma State University
in partial fulfillment of
the requirements for
the Degree of
DOCTOR OF PHILOSOPHY
May, 1980

RADIATION EFFECTS IN

QUARTZ RESONATORS

Thesis Approved:

Joel O. Martin
Thesis Adviser

Richard C. Bowell

Larry E. Halliburton

McG Rockley

W. A. Sibley

Norman N. Durham
Dean of the Graduate College

ACKNOWLEDGMENTS

It is a pleasure to acknowledge the advice and assistance of some of the many individuals who helped in the completion of this work. Special thanks go to Joel Martin, my Ph.D. committee chairman and major adviser, with whom it has been my pleasure to work over the last three years. Thanks too, to Bill Sibley and Larry Halliburton, for their continuing advice and enthusiasm on quartz and sundry matters. I would also like to thank the others who have worked on the quartz project at various times, Mark Markes, Nicholas Koumvakalis and Mary Wintersgill Fontanella, for their suggestions and contributions. I would like to acknowledge the sterling efforts of Mr. Heinz Hall and the Physics and Chemistry Instrument Shop, without whom life would have been a great deal harder. My appreciation goes to Dick Powell and Mark Rockley for their time and interest in this project, and for consenting to be on my Ph.D. committee.

Finally, I would like to extend my heartfelt thanks to my wife, Mary, to whom this thesis is dedicated, for her love, patience, and understanding during these three years out in the wilderness.

TABLE OF CONTENTS

LIST OF FIGURES

Figure Page

Figure Page

CHAPTER I

INTRODUCTION

Quartz, the crystalline form of silicon dioxide, occurs naturally in many parts of the world. From its earliest use in the form of flint to its current use in electronic systems aboard spacecraft and satellites, quartz has played an important role in the development of Man. Today quartz is used widely in electronics, from computers to digital watches and demand for it grows annually.

Alpha-quartz, which crystallizes in the trigonal system is a member of crystal class 18 (trigonal holoaxial) and its symmetry group is D_3 (3 2). The z, or optic axis, is the axis of three-fold symmetry. Quartz is piezoelectric because of its symmetry properties. The melting point of quartz is 1750°C, its density is 2.65×10^3 kg.m^{-3}, and its hardness is 7 on the Mohs' scale. At atmospheric pressure quartz undergoes a phase transition from the alpha (trigonal holoaxial) to beta (hexagonal) form at 573°C. Quartz is a relatively inert material and is insoluble in ordinary acid acids. It is only slightly soluble in water, but can be disolved by hydrafluoric acid, or hot alkaline solutions. Quartz can exist in both right and left handed forms. Right-handed quartz will rotate the plane of polarization

of polarized light propagating along the z-axis, in the clockwise direction.

Natural quartz, mined chiefly in Brazil, is used widely throughout the electronics industry, although for precision applications it is now being superceeded by hydrothermally grown synthetic quartz. The declining use of natural quartz is due to the large amounts of raw materi material needed to obtain small sections suitable for device fabrication, and the high impurity content of the final material.

Synthetic quartz is grown hydrothermally, i.e. from solution rather than from the melt, using natural quartz as the starting material (1). Hydrothermal growth is necessary because the principal applications of synthetic quartz require the alpha form, which must be maintained at temperatures below 573°C. Synthetic quartz is grown in large autoclaves at temperatures of about 340 - 370°C under 2000 atmospheres pressure. As quartz is only slightly soluble in water, mineralizers such as NaOH or Na_2CO_3 are added to the (natural quartz) nutrient solution to increase the solubility. The resulting impurities in synthetic quartz can come from the starting material, the mineralizer (s) and also from the autoclave walls. The overall impurity concentrations in synthetic quartz are at least an order of magnitude lower than for natural quartz (1).

Piezoelectricity and Quartz Resonators

Piezoelectricity, literally pressure electricity, was first discovered by the brothers Pierre and Jacques Curie in 1880. They showed that certain crystals (including quartz) when compressed in certain directions show positive and negative charges on certain portions of their surfaces which disappear when the pressure is removed (2). Piezoelectricity is defined as the electric polarization induced by mechanical strain in crystals belonging to certain crystal classes, the polarization being proportional to the strain and changing sign with it. The converse piezoelectric effect also exists where a crystal is strained when electrically polarized. Both effects arise from the same fundamental property of the crystal, i.e. that it is non-centrosymmetric, and both are reversible.

The piezoelectric properties of quartz enable its use in the construction of precision resonators, narrow band filters and SAW (surface acoustic wave) devices. To understand how a quartz oscillator works, consider a small rectangular bar of quartz with a pair of electrodes vapor deposited on opposite faces. The simplest mechanical mode of vibration of this bar is longitudinal. If an electric field is applied briefly to the electrodes, then the converse piezoelectric effect will cause a strain in the crystal which will continue as long as the electric field is applied. When the electric field is removed, the crystal will begin to relax mechanica-

lly to its equilibrium position, and then overshoot to its position of maximum strain in the negative direction. In this position, it will induce a voltage on the electrodes due to the piezoelectric effect, opposite in sign to that originally applied. The rectangular bar will continue to mechanically oscillate about its equilibrium position (like a damped harmonic oscillator) inducing an alternating voltage on the electrodes at the same frequency as the mechanical oscillations. Eventually the amplitude of the mechanical oscillations (and hence the induced alternating voltage) will decay to zero because of the mechanical damping of the system. This can be overcome by placing the quartz resonator into an electronic circuit that will start the resonator oscillating and supply energy to the resonator (via a feedback circuit) to compensate for its mechanical losses.

The frequency at which a resonator oscillates is known as its resonance, or resonant, frequency and for the narrow rectangular bar, the frequency of longitudinal vibration is given by:

$$f_r = \frac{1}{2a\sqrt{\rho s_{11}}} \qquad (1)$$

where a is the length of the crystal, ρ is the density and s_{11} is the inverse of Young's modulus along the bar.

Some important properties of a quartz resonator are its resonant frequency and Q (proportional to the sharpness of the resonance), its mode of vibration, e.g. shear, etc., and the temperature coefficient of its resonant frequency.

A number of different types of quartz resonators have been developed to overcome some of the shortcomings inherent in the simple rectangular longitudinal mode X or Y-cut crystal. These are illustrated in Figure 1 (3). One particular type, the rotated Y or AT-cut, has achieved widespread use because of its zero temperature coefficient.

The AT-cut resonator was developed during the 1940's as a result of investigation of the effects of rotating the angle of cut on the piezoelectric and elastic constants of quartz. Figure 2 shows the temperature coefficient as a function of rotation angle (about the x-axis) for a number of rotated Y-cut resonators (3). The temperature coefficient is zero at $35^{\circ}15'$ and -49°, which are known as the AT and BT cuts, respectively. These cuts have thickness shear modes of vibration giving greater freedom from unwanted modes and higher spectral purity than other styles of resonator.

Figure 3 illustrates the frequency versus temperature characteristics of three AT-cut resonators for which the angle of cut has been varied by a few seconds of arc (4). Precision resonators are cut at a rotation angle such that the frequency characteristic has a minimum at about $70^{\circ}C$. These resonators are then operated at that temperature in minature temperature-controlled ovens (to $0.1^{\circ}C$ or better). The frequency of the resonator is then unaffected by changes in the ambient temperature (which is typically $20 - 30^{\circ}C$) and only very slightly affected

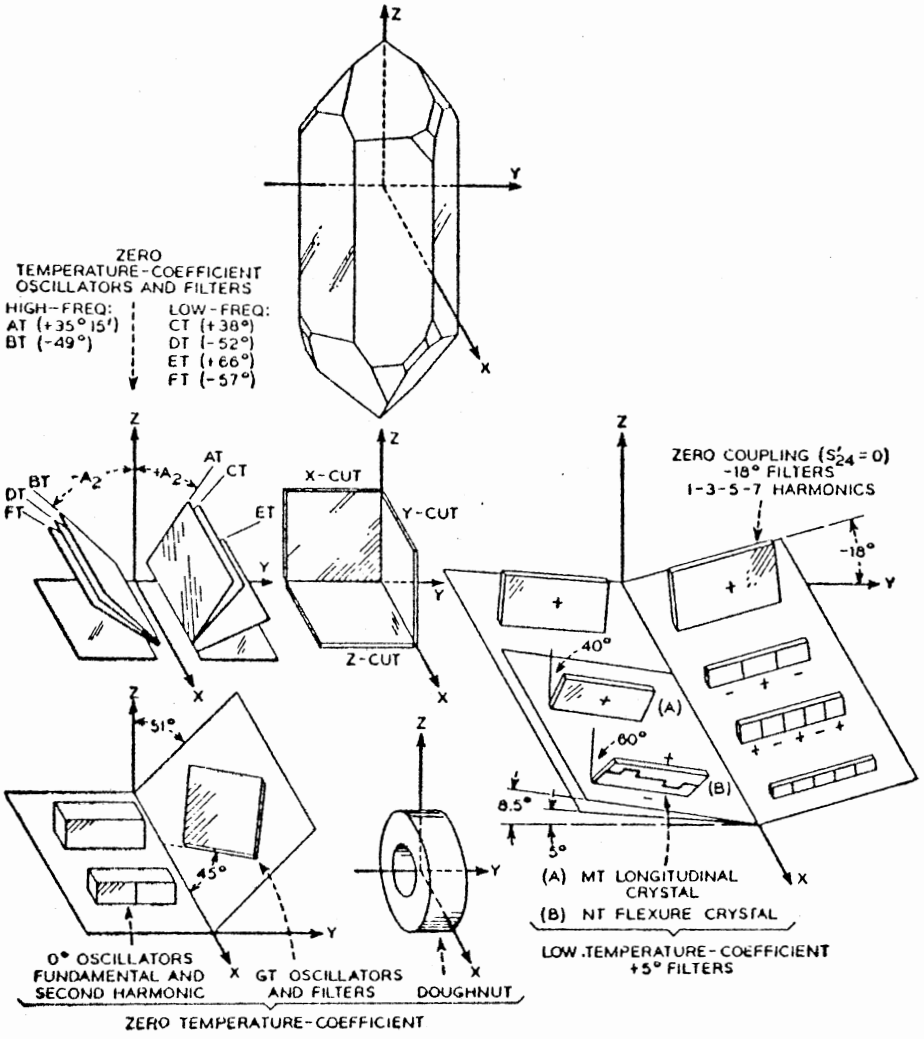

Figure 1. Quartz Crystal and Principal Cuts

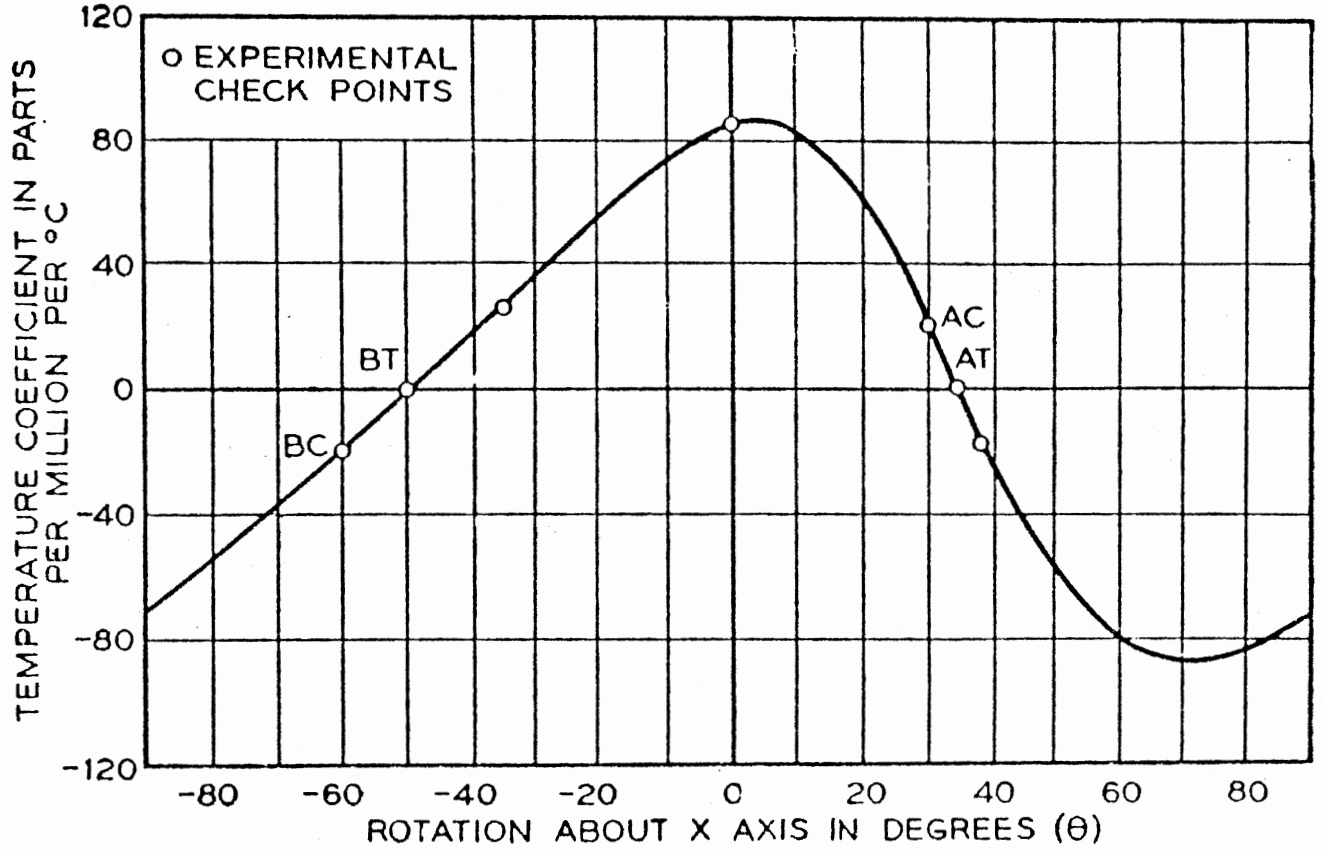

Figure 2. Temperature Coefficients for Rotated Y-Cut Resonators as a Function of Rotation Angle (about the x-axis)

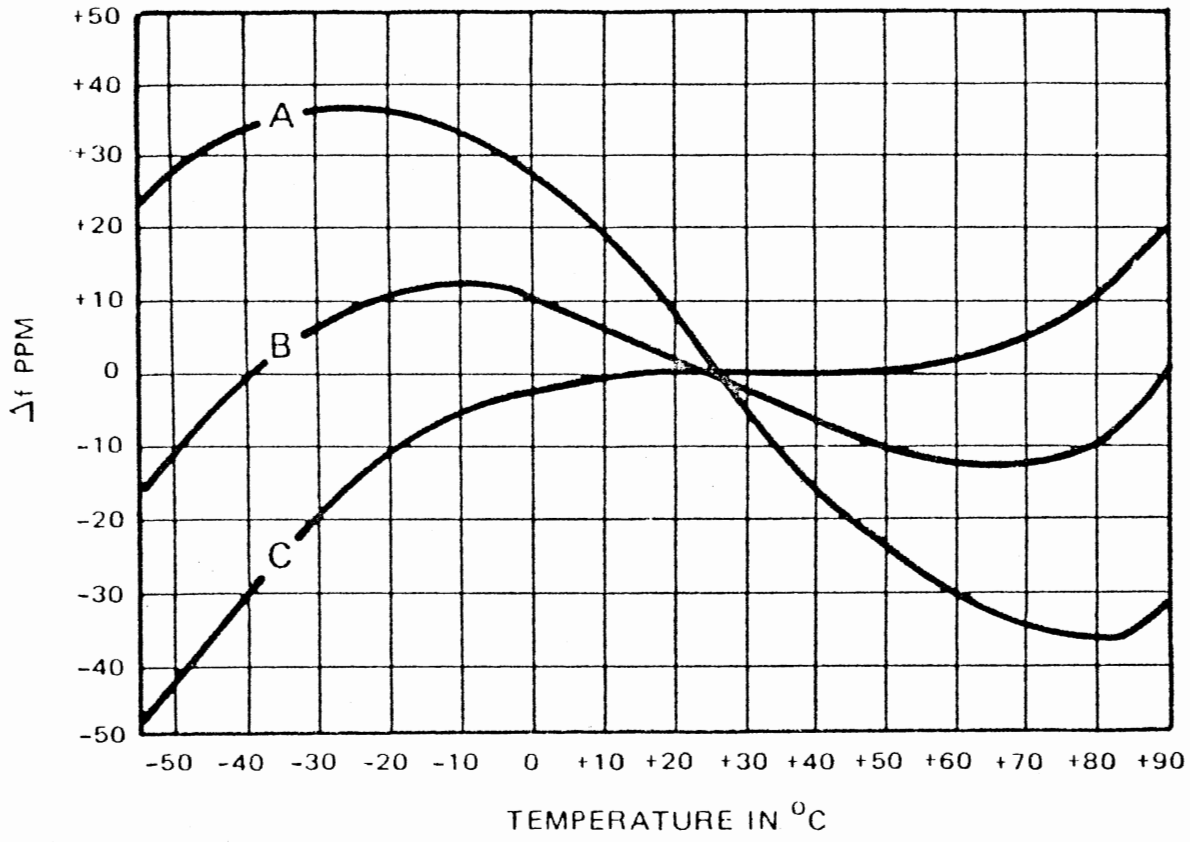

Figure 3. Frequency-Temperature Characteristics of AT-Cut Resonators whose Angle of Cut (about the x-axis) has been Varied by a few Seconds of Arc

(typically 10-100 ppb) by changes in the oven temperature.

The current industry-standard precision resonator is a 5 MHz 5th overtone (circular) plano-convex AT-cut quartz resonator. This type of resonator was used exclusivly during this study. The investigation of these precision resonators and their interaction with radiation involves measurement of their resonant frequency and Q as a function of temperature. The electrical equivalent of a quartz resonator is shown in Figure 4 (2-6). The reactance and impedance of this parallel RLC circuit as a function of frequency is given approximatly by:

$$X = (\omega L_1 - 1/\omega C_1) \qquad (2)$$

and

$$Z = (R_1^2 - (\omega L_1 - 1/\omega C_1)^2)^{\frac{1}{2}} \qquad (3)$$

respectivly. The reactance of the resonator as a function of frequency is shown in Figure 5. The points at which the reactance becomes zero are known as the series resonant (minimum impedance) and parallel resonant (maximum impedance) frequencies. In terms of the circuit parameters, these are given by:

$$f_s = \frac{1}{2\pi\sqrt{L_1 C_1}} \qquad \text{and} \qquad f_p = \frac{1}{2\pi\sqrt{\frac{L_1 C_1 C_o}{C_1 C_o}}} \qquad (4)$$

The transmission spectrum of the resonator (the impedance as a function of frequency) is shown in Figure 6. The Q of the resonator is defined as the series resonant frequency divided by its 3dB bandwidth.

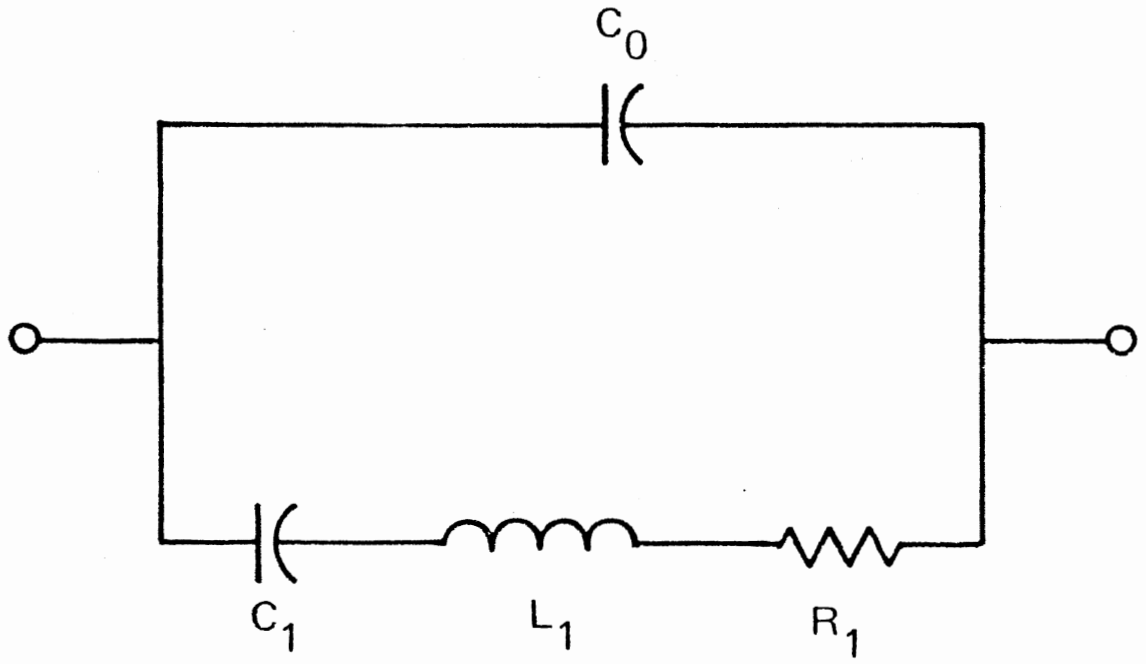

Figure 4. The Electrical Equivalent of a Quartz Resonator

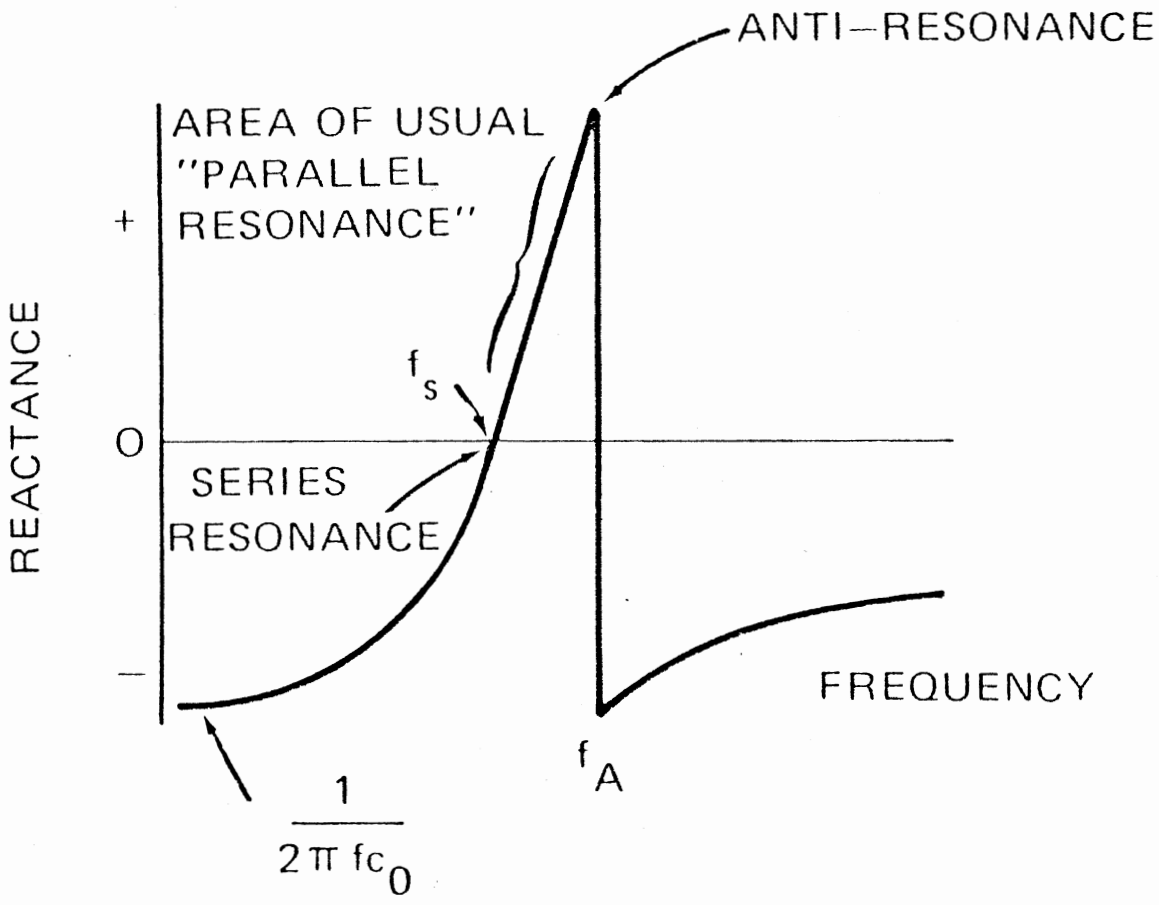

Figure 5. The Reactance of a Quartz Resonator as a Function of Frequency Illustrating the Series and Parallel Resonant Frequencies

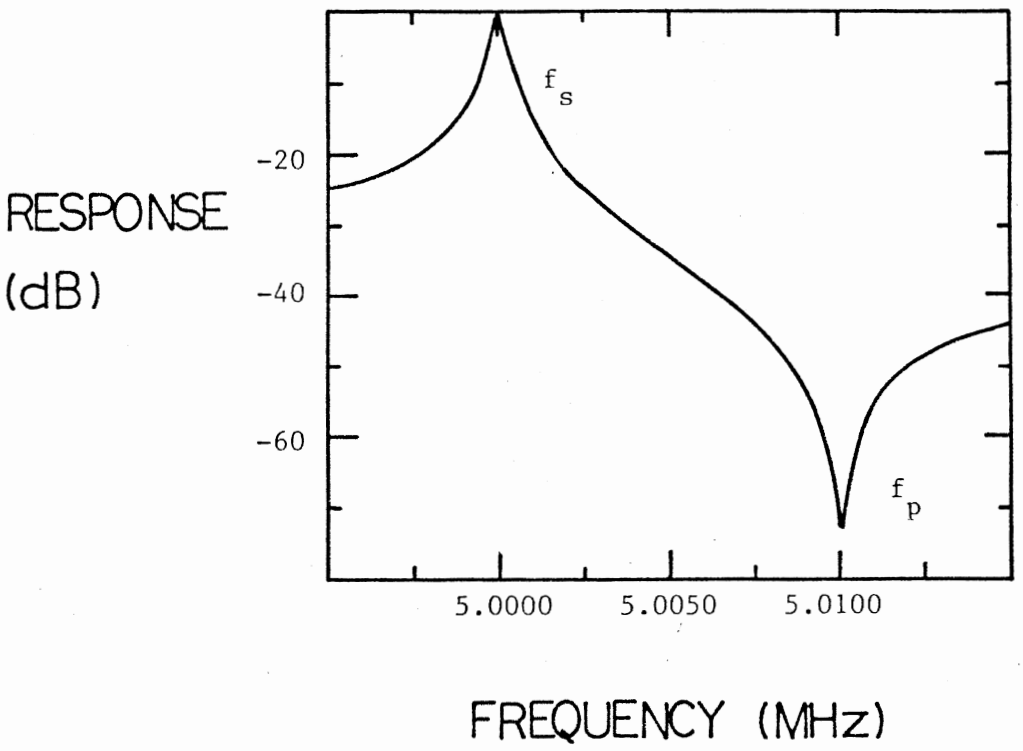

Figure 6. The Transmission Spectrum of a Quartz Resonator Showing the Normalized Impedance as a Function of Frequency

$$Q = f_s / \Delta f_{3dB} \tag{5}$$

$$= \frac{1}{2 f_s C_1 R} \tag{6}$$

$$= \frac{\omega_s L_1}{R} \tag{7}$$

where R is the total circuit resistance (6). The resonator can also be used as a filter. Examination of Figure 6 show shows that if a signal containing a number of frequrncies is passed through the resonator, only the component of the signal at the resonant frequency will be transmitted to any significant extent. The resonator is thus acting as a very sharp band-pass filter.

Measurements of the Q of a resonator are usually presented in the form of the inverse Q (Q^{-1}) as a function of temperature. The inverse Q is known as the acoustic loss and is directly related to the underlying loss mechanisms in the resonator.

Finally a brief note on nomenclature is appropriate at this point. The words resonator, resonator blank, and oscillator are often used synonymously in this study, though each has a specific meaning. After a piece of quartz has been fashioned into the form of a resonator, but before the electrodes and mounting hardware are attached, it is called a resonator blank, or simply a blank. It was in this form that the resonators were studied. After the electrodes are vapor deposited and the resultant assembly mounted in a hermetically sealed can, it is known

as a resonator. An oscillator describes an electronic circuit, containing a resonator, which gives a fixed frequncy sine or square wave output.

Defects in Quartz

Quartz, as all crystalline solids, can have both line and point defects in the lattice. Though this study is chiefly concerned with point defects, the role of line defects is important. Natural quartz can exist in both right and left-handed forms (often in the same crystal) and it is important for device applications to ensure that only one form is present. Another type of line defect is Dauphine, or electrical twinning, which occurs when alpha-quartz is cycled through the phase transition at 573 ^{o}C. Electrical twinning resulst from a 180^{o} change in the direction of the crystal atomic arrangements (2,3). Cycling a device (resonator, filter etc.) through the phase transition temperature generally results in its deterioration and failure.

The principal point defect in high quality-synthetic quartz is an Aluminum 3+ ion substituting for a silicon 4+ ion in the lattice. This substitution leads to local charge imbalance and the necessity to provide charge compensation for the Al^{3+} ion. Possible charge compensators include interstitial alkali ions such as lithium (Li^{+}) and sodium (Na^{+}) and also interstitial hydrogen (H^{+}) ions. The hydrogen ions are associated with the non-bonding p orbitals on neighbouring oxygen ions to form hydroxyl (OH^{-}) complexes.

Hole compensation of the Al^{3+} sites can occur following irradiation. Electron (and x-ray) irradiation forms electron -hole pairs within the lattice and if sufficient electron traps are avaliable, a hole can be trapped at one of the non-bonding p orbitals on an oxygen ion adjacent to an Al site.

The alkali-compensated aluminum ions are referred to as the $Al\text{-}Li^{+}$ and $Al\text{-}Na^{+}$ centers, respectively, while the proton -compensated defect is labelled the $Al\text{-}OH^{-}$ center. The hole compensated center has a special designation, $[Al_e+]^{o}$.

The major interstitial impurity in synthetic quartz is sodium stemming from the use of NaOH and Na_2CO_3 as mineralizers in the growth solution. By contrast, the principal impurity in natural quartz is often lithium (7). The determining factor in the interstitial impurity concentration is believed to be the aluminum concentration. The sum of the sodium, lithium, hydrogen and hole concentrations is taken to be equal to the total aluminum concentration. This relation is generally assumed to be valid though there does seem to be more hydrogen in the lattice than this accounts for. The Al content (as measured by infrared techniques) varies from 10^{15} cm^{-3} to 10^{17} cm^{-3}. Synthetic quartz which contains the lowest Al concentration will in general yield the highest quality resonators.

There are a number of other point defects in quartz whose concentrations are in general an order of magnitude or so lower than the four already listed. These include the

oxygen vacency centers, E', which are composed of an electron trapped at a negative ion vacancy. Three such defects have been observed in quartz, the E_1', E_2', and E_4' centers (9,10). Another defect is an interstitial hydrogen atom, H^o, which is stable to about 125 K (10).

Review of Acoustic Loss Literature

Systematic studies of the acoustic loss (Q^{-1}) of high frequency precision quartz resonators similiar to those used for frequency standards (11) began at the Bell Telephone Laboratories in 1955. Bommel, Mason,and Warner (12,13) measured the acoustic loss of several AT-cut resonators from 1.5 K to 300 K. They observed two large loss peaks situated at 20 K and at 52 K and measured their activation energies. The two loss peaks were attributed (incorrectly, as it turned out) to dislocation relaxations for the low temperature loss at 20 K and to oxygen vacancies for the higher temperature loss at 52 K.

The first major investigation of the effects of irradiation on natural and synthetic quartz resonators was reported by King (14). The acoustic loss peaks at 20 K and 50 K were again reported in 5 MHz AT-cut resonators fabricated from both natural and synthetic quartz. Following irradiation at room temperature the 50 K loss peak was removed and a new loss at 100 K was introduced. Annealing the resonators at 500 ^oC for several minutes restored the 50 K loss to its original value. The technique of electrodiffusion (sweeping)

was introduced by King in an attempt to increase the radiation hardness of the resonators.

Jones and Brown (15), in a study of the effect of growth rate on the 20 K and 50 K acoustic loss peaks, found an increase in the 50 K loss with increasing growth rate. In studies of the effects of irradiation on the internal friction (Q^{-1}) in synthetic quartz (16), they found again that irradiation with x-rays at room temperature removed the 50 K loss peak and annealing above 450 ^{o}C restored it. Their explanation of the defects underlying the 20 K and 50 K loss peaks was given in terms of the previously reported models of Bommel et al. (12,13).

A major advance in the understanding of the defect mechanisms in quartz was reported by Fraser in 1964 (17). He used the electrodiffusion technique to sweep lithium, sodium, and potassium ions into three identical blocks of natural quartz from which resonators were subsequently fabricated. The loss peak at 50 K was shown to be due to sodium. The loss peaks at 105 K and 210 K were attributed to lithium and potassium, respectivly. In addition, a further loss peak at 140 K was linked to the presence of sodium. The large loss at 20 K was not found to be related to the alkali content, but was presumed to be due to a phonon-phonon interaction proposed by Mason and Bateman (18).

The effect of pulsed ionizing radiation on selected quartz resonator crystals was examined by Poll and Ridgway (19). In natural quartz the radiation caused large frequency

shifts (which partially saturated for radiation doses greater than $3x10^5$ Rads) along with a sharp transient loss in the resonator Q. In all cases the effects of irradiation were greatest on the resonators fabricated from natural quartz as opposed to synthetic quartz. Flanagan and Wrobel (20) also studied the effects of irradiation on the oscillator frequency.

The majority of the studies of the effects of irradiation on the transient and steady state frequency offsets were inconclusive and inconsistant. This was mainly due to the wide difference between resonators used, both in terms of their origins and their impurity concentrations.

Capone, Kahan, Brown and Buckmelter (21) investigated radiation effects in a number of high Q 5 MHz 5th overtone AT-cut resonators fabricated from natural and synthetic quartz which had undergone various treatments. The resonators were fabricated under nearly identical manufacturing conditions. This study is important because it looked at the frequency shifts following irradiation (at the normal operating temperature of the oscillators) and then went on to measure the acoustic loss as a function of temperature from 4 K to 475 K. The study attempted to explain the various observed offsets in terms of the changes in the acoustic loss and ultimately in terms of the behavicur of the defects and impurities present in the quartz.

The reduction of the 50 K sodium loss peak upon room temperature radiation was observed by Capone et al., as

well as a broad increase in the acoustic loss in the 250 - 300 K region for natural and lithium-doped quartz. The best material studied i.e. the most radiation resistant was swept Electronic Grade quartz. Swept Electronic Grade resonators showed higher Q values in the 200 - 400 K range, no sodium loss peak at 50 K, and a reduced 20 K phonon-phonon loss. The effects of electron irradiation to 1 MRad were extremly small and lay within the experimental error of the Q measurements.

In this investigation by Capone et al., all the resonators studied showed a number of loss peaks in the 120 - 180 K range which were attributed to coupled modes. These coupled modes, also referred to as interfering modes or mode crossings, are believed to be the result of the interaction of two distinct modes of oscillation within the crystal. This interaction takes place over a narrow temperature range of about 5 - 10 K. The frequency-temperature characteristic of the interfering mode appears to be quite different to that of the principal mode, intersecting it just at the mode crossing. However since the Q curves of both modes of vibration are not infinitly sharp (see Figure 6), there will be a small temperature range in which the two curves overlap. This overlap between the two Q curves means that if the resonator is excited by an rf pulse whose frequency lies within this pass-band, both modes of vibration will be simultaneously excited. The effect will be to give a composite decay which will contain the sum and difference frequencies

of the two modes of vibration. The actual decay observed near the temperature at which a mode crossing occurs is non-exponential and possesses a beat structure. The shape of the decay varies rapidly as the frequency of the exciting pulse is varied slowly through the pass-band of the resonators interfering mode response.

King and Sander(22-24) in a series of studies have looked at the transient changes (in Q and frequency) of 5 MHz and 125 MHz overtone resonators following pulsed irradiation. Amoung the conclusions found was that a transient post-irradiation negative frequency offset occured which annealed with a $t^{-\frac{1}{2}}$ dependence. The resonator Q was observed to decrease sharply following pulsed irradiation, proportional to dose and inversely proportional to frequency. They proposed that the initial frequency offset in pulse irradiated quartz resonators is due to the radiation-induced mobility of hydrogen ions from substitutional Al sites. The subsequent annealing of the offset is then believed to be due to recombination of the hydrogen ions at the Al sites, reforming the $Al\text{-}OH^-$ center. The acoustic loss peak observed at 100 K is postulated as being associated with the $[Al_e^+]^o$ center.

Fraser (7) provides a good general review article in which the effects of sweeping and irradiation on 5 MHz 5th overtone AT-cut resonators are discussed. Weil (25) has compiled a comprehensive literature review of investigations of Al-related defects in alpha-quartz.

Project and Thesis Outline

This study is part of a larger project undertaken at Oklahoma State University from June 1977 to November 1979. The project involved a detailed, systematic investigation of the effects of ionizing radiation on quartz resonators and resonator material using acoustic, magnetic and optical measurements. ESR, optical and infrared absorption, and luminescence techniques were used as microscopic probes of the defects introduced into the quartz resonator (or an adjacent piece of the original ingot) during irradiation. The technique of electrodiffusion (sweeping) was investigated as a method of increasing the radiation hardness of the quartz resonators, and also as a method of enhancing the concentration of selected ions (Li^+, Na^+, H^+, and holes) for defect identification studies.

This project is unique in that it involves infrared, ESR, and acoustic loss (Q^{-1}) measurements on identical (or adjacent) pieces of well characterized quartz. The results obtained from one technique can thus be directly correlated with those from other techniques, as the measurements were made on identical samples. High quality commercially grown Electronic Grade and Premium Q z-growth lumbered bars were used throughout the study.

The principal goals of this thesis are the identification of the defects giving rise to the acoustic loss peaks in 5 MHz 5th overtone AT-cut quartz resonators and their

steady state behaviour following irradiation in the temperature range 77 K - 300 K. Electrodiffusion (sweeping) and thermal annealing techniques are also used in efforts to characterize the loss peaks.

CHAPTER II

ANELASTICITY AND ACOUSTIC LOSS : A REVIEW

The stress-strain relationship in a perfectly elastic crystal is given by Hooke's law

$$S = JT \tag{1}$$

where S is the strain, T is the applied stress and J is the modulus of compliance or just the compliance. However, many materials deviate from perfect elasticity in their behaviour. One method of describing such non-ideal materials is by treating them as anelastic solids (26-28). An anelastic solid is defined as one for which the instantaneous and single valued features of Hooke's law are discarded but the linearity and unique equilibrium relationship features are retained (27). Specifically an anelastic solid exhibits the following features, (i) for every stress there is a unique equilibrium value of strain (and visa versa), (ii) the equilibrium response is only achieved after the passage of sufficient time, and (iii) the stress-strain relationship is linear. Hooke's law for an anelastic solid can now be written as

$$aT + b\dot{T} = cS + d\dot{S} \tag{2}$$

where $\dot{T}$ and $\dot{S}$ are the time derivatives of the stress and strain respectivly. This equation can be rewritten as

$$J_R T + \tau_T J_u \dot{T} = S + \tau_T \dot{S} \tag{3}$$

To look at the effects of anelastic behaviour in various materials it is necessary to solve this differential equation for different boundary conditions corresponding to the different types of experiment e.g. static, dynamic etc. For a piezoelectric quartz resonator the applied stress has a sinusoidal time dependence

$$T = T_o \exp(i\omega t) \tag{4}$$

The strain however, is not generally in phase with the applied stress when relaxation effects are present, but will lag by a phase angle ϕ.

$$S = S_o \exp(i(\omega t - \phi)) \tag{5}$$

$$= (S_1 - iS_2)\exp(i\omega t) \tag{6}$$

S_1 and S_2 are the components of strain in phase and out of phase, respectivly, with the applied stress. The relationship between strain and stress in this experiment can be written as

$$S = J^* T \tag{7}$$

where J^* is the complex compliance, which is in general a function of ω, and can be expressed in terms of its real

and imaginary parts:

$$J^*(\omega) = J_1(\omega) - iJ_2(\omega) \tag{8}$$

where $$J_1(\omega) = \frac{S_1}{T_o} \quad , \quad J_2(\omega) = \frac{S_2}{T_o} \tag{9}$$

and $$\tan\phi = \frac{S_2}{S_1} = \frac{J_1}{J_1} \tag{10}$$

If the expressions for the time dependences of S and T are substituted into the differential equation for the standard anelastic solid, then the following relations for $J_1(\omega)$ and $J_2(\omega)$ result

$$J_1(\omega) = J_u + \frac{\delta J}{1 + \omega^2\tau_T^2} \tag{11}$$

$$J_2(\omega) = J_\bullet \frac{\omega\tau_T}{1 + \omega^2\tau_T^2} \quad . \tag{12}$$

These are the well known Debye equations. The function $J_2(\omega)$, when plotted as a function of $\log\omega\tau_T$, yields a symmetric peak about $\omega\tau_T = 1$ as shown in Figure 7.

The phase angle ϕ, more usually expressed as $\tan\phi$, is called the internal friction and is a measure of the internal loss in the material. It too can be written in the form of a Debye equation

$$\tan\phi = \frac{\Delta}{(1 + \Delta)^{\frac{1}{2}}} \cdot \frac{\omega\tau_r}{1 + \omega^2\tau_r^2} \tag{13}$$

where $\Delta = (\delta J/J_u)$ is a dimensionless measure of the relaxat-

ion strength and

$$\tau_r = \tau_T (J_u/J_R)^{\frac{1}{2}} = \tau_T (1+\Delta)^{-\frac{1}{2}} \qquad (14)$$

The Debye peak for tanø is centered at $\omega\tau_r = 1$ rather than $\omega\tau_T = 1$. Since $\Delta > 0$ and usually $\ll 1$, $\tau_r \sim \tau_T$ and the equations are usually written without a subscript.

It can be seen that for a standard anelastic solid the measurable functions $J_1(\omega)$, $J_2(\omega)$, and tanø take on particularly simple forms when plotted against $\log \omega\tau$. Here it has been assumed that the experiment is being performed at constant temperature with the relaxation time τ being kept constant while the frequency of the applied stress, ω, is varied. For a quartz resonator which will only resonate at certain fixed frequencies (the fundamental and overtone frequencies), it is necessary to perform the complimentary experiment where ω is kept constant while τ is varied. This is accomplished by assuming that the loss mechanism that gives rise to $J_2(\omega)$ is thermally activated and follows an Arrhenius relation of the form

$$\tau = \tau_o \exp(\Delta H/kT) \qquad (15)$$

where ΔH is the enthalpy of activation of the loss. This relation implies

$$\ln(\omega\tau) = \ln(\omega\tau_o) + (\Delta H/k)(1/T) \qquad (16)$$

Hence a plot of $J_2(\omega)$ and tanø(ω) against $(1/T)$ will also yield a Debye type peak. For small defect concentrations,

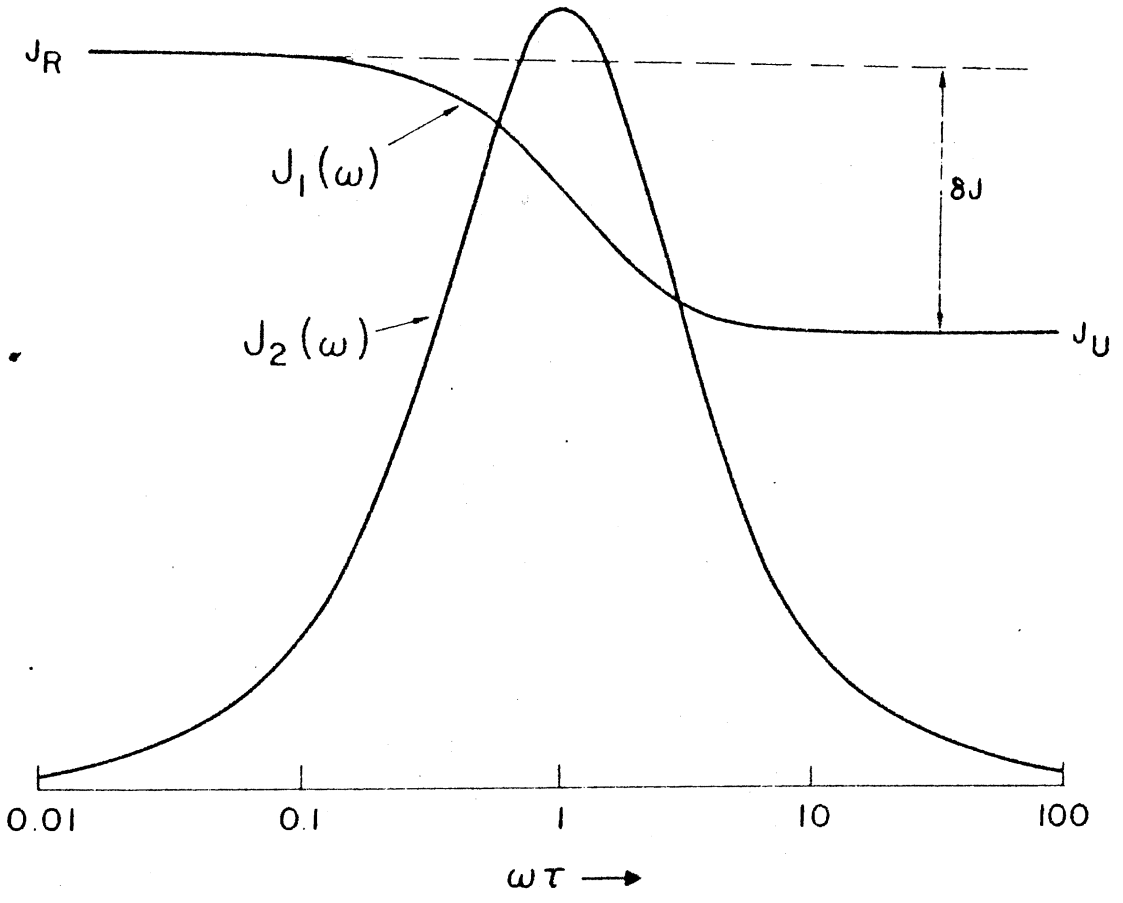

Figure 7. The In-Phase and Out-of-Phase Components of the Complex Compliance, J_1 and J_2, as a Function of Log $\omega\tau$ where ω is the Angular Frequency of the Applied Stress and τ is the Relaxation Time (at Constant Stress)

δJ and Δ vary slowly with (1/T) so a plot of $T\tan\phi$ versus (1/T) will yield a more symmetric peak.

Measurement of the resonator Q is directly related to the internal friction

$$Q^{-1} = \tan\phi(\omega) = D \cdot \frac{\omega\tau}{1 + \omega^2\tau^2} \quad . \tag{17}$$

At the temperature at which the maximum loss (minimum Q) occurs, $\omega\tau = 1$ and so

$$Q_{max}^{-1} = D/2 \tag{18}$$

and

$$Q^{-1} = 2Q_{max}^{-1} \cdot \frac{\omega\tau}{1 + \omega^2\tau^2} \quad . \tag{19}$$

The resonant frequency of an AT-cut quartz resonator is given by

$$f = \frac{1}{2t} (c'_{66}/\rho)^{\frac{1}{2}} \tag{20}$$

where

$$c'_{66} = c_{66}\cos^2\theta + c_{44}\sin^2\theta - c_{14}\sin 2\theta \tag{21}$$

and θ is the angle of rotation of the cut about the x-axis ($35^\circ\ 15'$ for the AT-cut). Any change in the resonant frequency is related to changes in the stiffness coefficients c_{ij}.

$$\frac{\Delta f}{f} = \frac{1}{2} \cdot \frac{d(c'_{66})}{c'_{66}} \tag{22}$$

If there is a change in the acoustic loss, Q_{max}^{-1}, e.g., after

irradiation, then there will be a corresponding change in the frequency

$$\frac{\Delta f}{f} = \frac{D}{2} = Q_{max}^{-1} \tag{23}$$

The acoustic loss (Q^{-1}) of the resonators used in this study was measured by means of the pulsed or logarithmic decrement method. This technique involves pulsing the crystal briefly at its resonant frequency and observing the free decay. The differential equation which describes the resulting motion is (27)

$$m\ddot{x} + k_1(1 + i\tan\phi)x = 0 \quad . \tag{24}$$

The solution of this equation which describes the free vibration in the presence of internal friction is of the form

$$x = x_o \exp(i\omega^* t) \tag{25}$$

where $$\omega^* = \omega_o(1 + (i\delta/2)) \tag{26}$$

and $$\delta \simeq \pi\phi \tag{27}$$

This can be written as

$$x = x_o \exp(i\omega_o t)\exp(-\delta\omega t/2) \tag{28}$$

$$= x_o \exp(i\omega_o t)\exp(-\delta f t) \tag{29}$$

$$= A(t)\exp(i\omega t) \tag{30}$$

which describes exponentially damped oscillations (at ω_o) if δ is small. The dimensionless quantity, δ, can be found from the ratio of the amplitudes of sucessive vibrations

$$\delta = \ln(A_n/A_{n-1}) \tag{31}$$

and is known as the logarithmic decrement.

The acoustic loss is found from the time constant of the free decay of the resonator following excitation at its resonant frequency. The envelope of the sinusoidally decaying voltage is given by

$$V = V_o \exp(-t/t_o) \tag{32}$$

where t_o is the time constant of the decay and is equal to $t_{\frac{1}{2}}/\ln(2)$. Comparing this with the expression derived above for the envelope

$$x = x_o \exp(-\delta f t) \tag{33}$$

$$\delta f = 1/t_o \tag{34}$$

but $$\delta \sim \pi\phi \sim \pi\tan\phi \sim \pi Q^{-1} \qquad (\phi \text{ small}) \tag{35}$$

so $$\pi f Q^{-1} = 1/t_o \tag{36}$$

hence $$Q^{-1} = \frac{1}{\pi f t_o} \quad . \tag{37}$$

CHAPTER III

EXPERIMENTAL TECHNIQUES

Resonator Fabrication and Mounting

Five MHz 5th overtone AT-cut quartz resonator blanks were used exclusively in this study. A number of resonators were supplied by Dr. Alton Armington of RADC (29). The remaining resonators used in this study were fabricated by either Kansas Crystal Company (30) or K-W Manufacturing (31) from pure Z growth lumbered bars of synthetic quartz purchased from Sawyer Research Products Inc. (32). The resonators were fabricated to specifications given by Fraser (7).

The resonators were not plated but were excited in a contactless holder using a parallel plate type arrangement. Three versions of sample holder were used in this study. In the first holder, illustrated in Figure 8, the resonator was mounted horizontally and held in place by gravity. This arrangement provided good thermal contact between the resonator and the copper holder. The resonator was excited electrically between the upper electrode on the printed circuit board and the copper base of the holder. During this phase, a glass cryostat was utilized and irradiations were accomplished by removing the resonator from it's

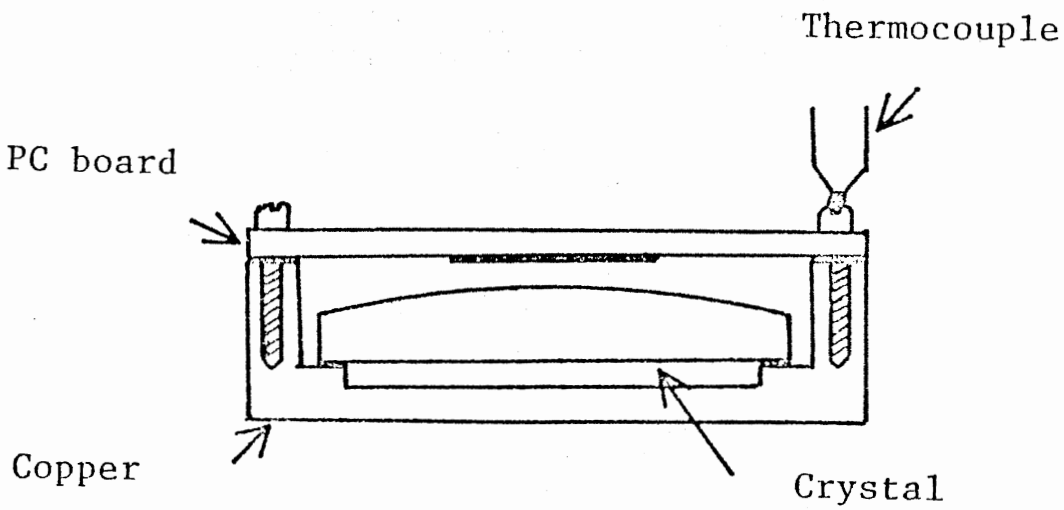

Figure 8. Horizontal Resonator Mounting

holder, irradiating it, and then remounting it in the holder. This procedure proved unwieldy during the main phase of the study when it was necessary to perform variable temperature irradiations in the range 77 K - 300 K.

To accomplish variable temperature irradiation, a stainless steel cryostat was designed and constructed. This cryostat, which had Al windows and an angled mounting system for the resonators (to allow irradiation), allowed two resonators to be measured at the same time. This greatly increased the amount of data that could be obtained in a given time. The major disadvantage of this angled mounting system was that the resonators did not make good thermal contact with the holder and were easily knocked out of alignment. These problems were overcome by using a thermal epoxy glue to fasten three small tabs to the resonator (along the x and z' directions). This allowed the resonators to be clamped into the holder, securing them in place. In addition, instead of bringing the cryostat to the Van de Graaff generator for irradiation with 1.5 MeV electrons, a 50 keV X-ray generator was used to irradiate the resonators in situ.

The final mounting system developed during the third phase of the study consisted of two horizontal holders mounted one on top of the other. An Al radiation window was placed in the cryostat beneath the sample area to allow X-irradiation from below. This holder worked very well giving extremely high resonator Q's at liquid helium temp-

eratures (Q 10^7-10^8). The resonators were operated in a vacuum of about 10^{-5} Torr.

Variable Temperature Cryostat

A stainless steel variable-temperature cryostat was designed for this study (32) and constructed in the Physics and Chemistry Instrument Shop under the very capable direction of Heinz Hall. This cryostat enabled measurements of the Q and resonant frequency of two resonators (at a time) to be made over the range 4 K - 400 K. The cryostat consisted of an inner and outer Dewar system, vacuum insulated from the surroundings. The inner Dewar could be filled with either liquid nitrogen or liquid helium. This cryostat exhibited excellent thermal characteristics at liquid helium temperatures as a fill of 1.25 l of liquid helium would last in excess of 8 hours with the sample temperature progressively raised from 4 K to 77 K.

The temperature control system consisted of a HP 610B power supply driving a 14Ω constantan heater wrapped around the cold finger of the cryostat. The temperature was monitored using a Digitec 268 digital millivoltmeter to measure the emf of an ice-referenced gold-iron (7%): chromel thermocouple. Temperature control was accomplished by setting the power supply voltage (applied to the constant heater load) with a Microtona DVM which then maintained the sample assembly at a constant temperature (say 100 K). To make a measurement at the next higher temperature (104 K),

the power supply voltage was increased to 2-2.5 times its equilibrium value. The temperature was allowed to rise exactly three degrees (to 103 K) and the power supply voltage was reduced to the previous equilibrium value plus 0.1 V. The temperature would then continue to rise, reaching an equilibrium value 4 K above the initial value in 8-10 minutes. This scheme, though crude, worked well allowing the temperature to be set to within 0.2 K (under steady state conditions) with temperature stabitities of the order of 0.2 K / 5 minutes.

The heat leak chamber, which connected the sample assembly on the cold finger with the cryogenic fluid in the inner Dewar, was filled with helium gas and pumped on continuously (with a rotary pump) while the temperature was varied. To cool the sample assembly from room temperature to 77 K, for example, the heat leak chamber was first filled with a small amount of helium gas (at room temperature). Liquid nitrogen is then poured into the inner Dewar and the sample temperature rapidly falls to 77 K. When this temperature is achieved, the heat leak chamber is pumped out, partially disconnecting the sample chamber from the bath. This allows the use of lower heater powers to achieve a given temperature, prolonging the lifetime of the cryogenic fluid in the bath. Continuous pumping on the heat leak chamber with a rotary pump is crucial for stable and repeatable temperature control.

Acoustic Loss Measuring System

The acoustic loss of the resonators was measured using the logarithmic decrement technique. In this method, the resonator is excited at its resonant frequency for about 10 ms, then allowed to decay. The time constant of the envelope of the decaying waveform yields the resonator Q

$$Q^{-1} = 1/\pi ft \qquad (1)$$

where f is the resonant frequency and t is the time constant of the decay ($t_{\frac{1}{2}}/0.6931$). The resonant frequency is found by varying the exciting frequency until the largest amplitude decay results.

The block diagram of the system is shown in Figure 9. The output of the synthesizer (Exact model 801) at 5 MHz is applied to the rf gate which is opened for 10 ms every 1, 2 or 5 s by the pulser. This synthesizer output also goes to the 50 input of the frequency counter (HP 5326A Timer-Counter). The auxiliary output of the synthesizer at 5 - 30 MHz is mixed with a crystal-controlled offset oscillator which has a frequency of 29.545 MHz, to produce a difference frequency of 5.455 MHz. This is exactly 455 kHz above the frequency being applied to the resonator and tracks with it. This is equivalent to the local oscillator (LO) in a radio. After the resonator has been excited, it decays exponentially at its resonant frequency near 5 MHz. This decaying radio frequency voltage is then amplified by a wide-band pre-

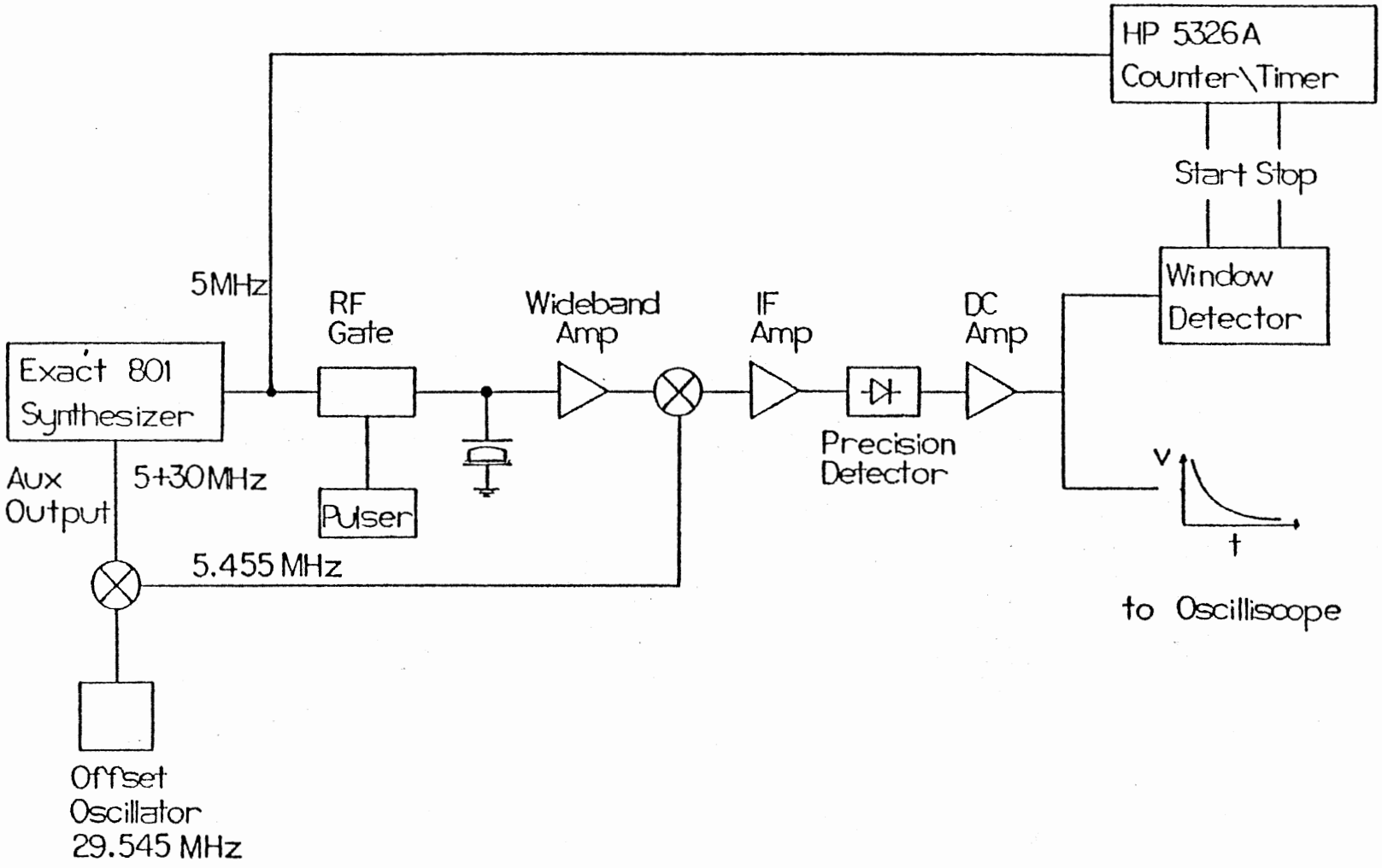

Figure 9. The Block Diagram of the Logarithmic Decrement Measuring System

amplifier and mixed with the 5.455 MHz LO output in a double-balanced mixer. The difference gives an exponentially decaying waveform at 455 kHz, which in radio terms would be called the intermediate frequency (IF). The IF signal is then amplified and detected (at 455 kHz) using a precision rectifier circuit. The output from the final DC amplifier is an exponential decay which is fed to a Tektronix 5441 variable persistance storage oscilliscope and to the window detector circuit. The storage oscilliscope is vital to this scheme allowing the decays to be monitored while varying the frequency to obtain series resonance. In addition, the oscilliscope provides a quick visual check of the exponential character of the decay, non-exponential decays indicate the presence of interfering modes.

The window detector circuit is the heart of the Q^{-1} measuring system and measures the time for the decay to fall from a (fixed) upper voltage level to a (variable) lower voltage level. The lower voltage level is usually set at half of the upper level so that the counter-timer when in the timer mode reads the half-time of the decay directly. The lower voltage level can be varied from 0.1to 0.9 of the upper level in 0.1 steps allowing a least squares fit to be made to check the exponential character of the decay. Using the oscilliscope, the size of the decay is adjusted with a variable attenuator so that the initial portion of the decay is set at the 90% graticule with the base line on the graticule corresponding to -10%. In this scheme, the

upper voltage level is at the graticule corresponding to 70%. For consistent measurements, these settings should be maintained.

The measurement sequence is as follows. At a stable temperature the synthesizer frequency is varied until the largest decay is observed on the oscilliscope. The height of the decay is then adjusted using the attenuator until it fits within the limits as outlined above. After the resonant frequency is recorded, the counter-timer is switched to the timer mode. The half-time of the decay is noted and the timer is switched to the time interval average mode (10 measurements). The average time for the 10 measurements is then recorded. Finally the temperature is increased as already outlined. Measurements are taken at 15 - 20 minute intervals depending on the temperature region in which the measurements are being made.

Irradiation Facilities

The irradiation facilities at Oklahoma State University consisted of a Van de Graaff electron accelerator and a 60 kV (maximum) X-ray generator. Initially, irradiations were carried out with 1.7 MeV electrons at beam currents of about 0.2 uA/cm^2 on the sample. Typical doses were approximatly 2000 J/cm^3 (10^8 Rads). Later, 50 keV X-rays were used for in situ irradiations at temperatures from 77 K to 300 K. Both facilities gave comparable radiation damage with the Van de Graaff accelerator being used for

about two minutes and the X-ray generator for about 1½ hours. The doses involved are not expected to produce significant amounts of knock-on damage but they have been shown to saturate the impurity-related defects observed in quartz (10).

Electrodiffusion (Sweeping) Facilities

The sweeping facility is illustrated schematically in Figure 10. The electrodiffusion process, in which selected ions are swept in or out of quartz by means of an electric field at elevated temperatures, takes place within a glass enclosure under vacuum or in a specific atmosphere, e.g. H_2. The electric field is applied to the bar of quartz (or resonator blank) by means of a pair of graphite electrodes using a Kepco APH 2000M high voltage power supply. When sweeping the circular plano-convex resonators directly, a piece of aluminum foil is placed between the curved side and the graphite electrode to ensure better electrical contact. The sweeping current is monitored by means of a Heath/Schlumberger strip chart recorder. The resonators were usually swept at 500 - 525°C with an applied voltage of 450 V (equivalent to an electric field of about 2100 V/cm across the sample). Resonators or bars of quartz were swept for a minimum of 24 hours.

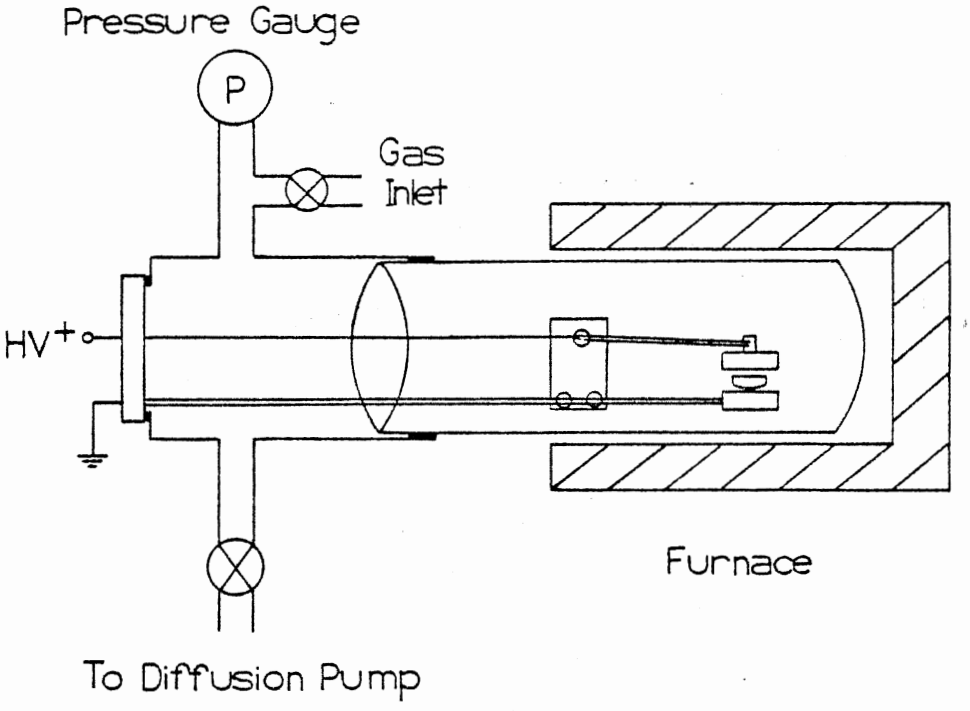

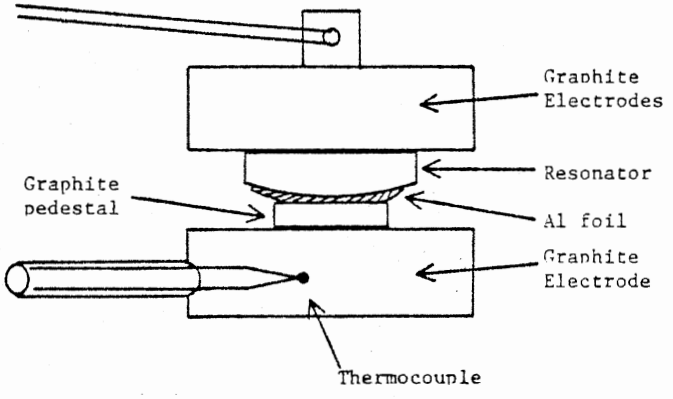

Figure 10. The Electrodiffusion (Sweeping) System

CHAPTER IV

RADIATION EFFECTS IN SWEPT ELECTRONIC GRADE QUARTZ

Introduction

The purpose of this chapter is to introduce the main features in the acoustic loss of a quartz resonator over the temperature range 4 K - 300 K. The resonator studied, EG-X 3(1), was fabricated from Electronic Grade quartz, swept by Sawyer Research Products Inc. (SARP I process) and supplied by Dr. A. F. Armington (29). The as-received acoustic loss spectrum and the frequency-temperature characteristics are presented and discussed. The acoustic loss spectra following two irradiations at room temperature are also shown. The effects of irradiation on the principal loss peaks are illustrated and possible models are discussed in terms of the known defects in swept Electronic Grade quartz.

The acoustic loss for resonator EG-X 3(1) as a function of temperature from 4 K to 300 K is shown in Figure 11. The resonator was mounted horizontally with no mechanical attachments (leading to the very high Q values below 10 K) in the glass cryostat system described in Chapter III.

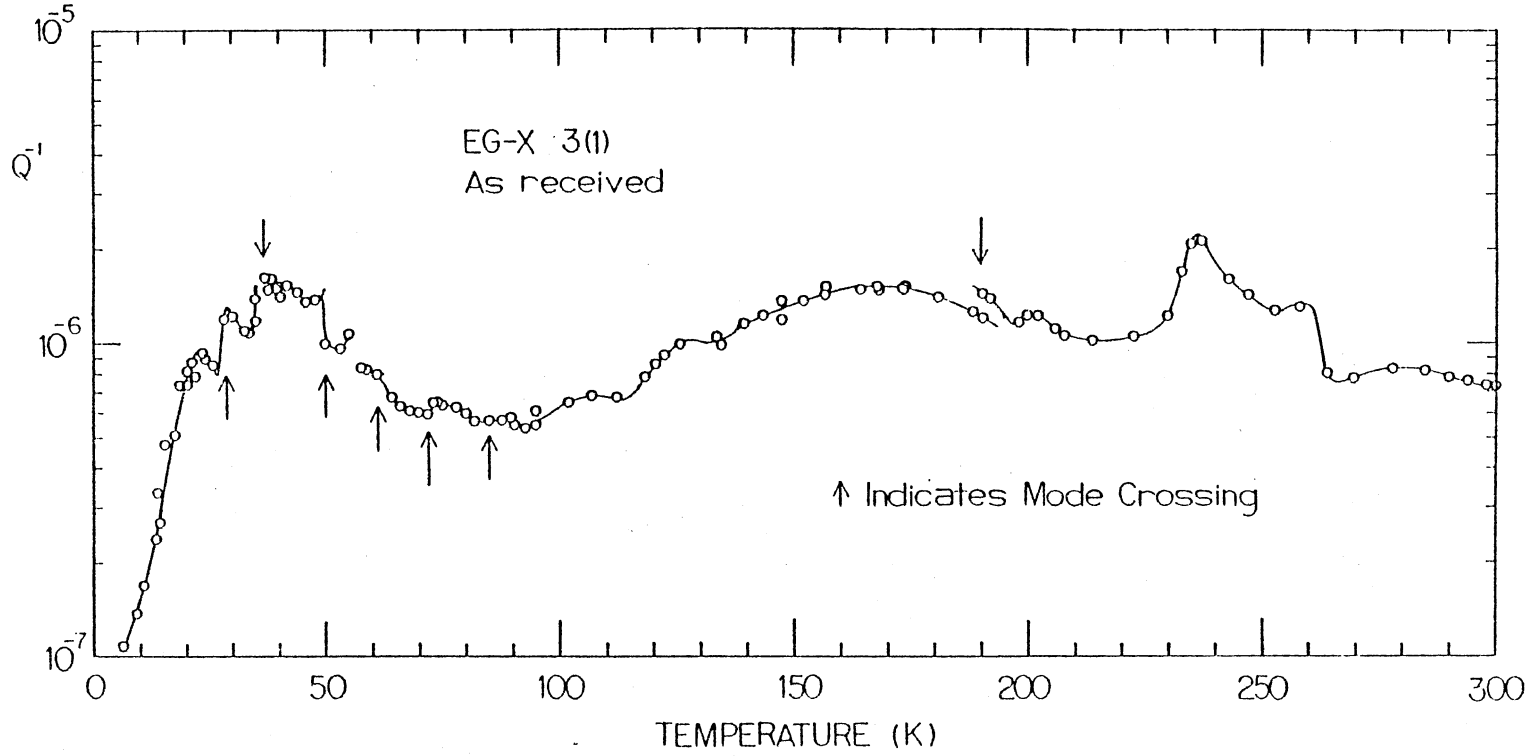

Figure 11. The Acoustic Loss Spectrum from 4 K - 300 K for As Received Swept Electronic Grade Resonator EG-X 3(1)

As the temperature is raised above 4 K the acoustic loss increases sharply, peaking at about 23 K. This loss peak is observed in all quartz resonators and is attributed to scattering between the thermal phonons and the 5 MHz shear vibrations. The strength of the coupling between the energy in the acoustic (shear) waves and the thermal phonons in the lattice is greatest around 23 K (18).

Between 25 K and 50 K, there are a number of sharp loss peaks which are due to interfering, or coupled modes, and are highlighted in Figures 11 and 12. These loss peaks (described in Chapter I) can be distinguished from 'real' loss peaks by the shape of the decay observed on the oscilloscope, and from the slope of the frequency-temperature curve. Near the temperature at which a mode crossing, or interfering mode occurs, the decay becomes distinctly non-exponential, and will often have a beat structure superimposed on it. The frequency-temperature curve plotted in the normalized form, $(f_T - f_{300})/ f_{300}$ against temperature exhibits a discontinuity in the same temperature range. This is illustrated in Figure 12. The mode crossing at 190 K is particularly striking in both the frequency and acoustic loss figures. Resonators can be fabricated which are free of interfering modes over a narrow temperature range, but it is probably impossible to manufacture resonators which will show no spurious responses over as wide a temperature range as 4 K to 300 K.

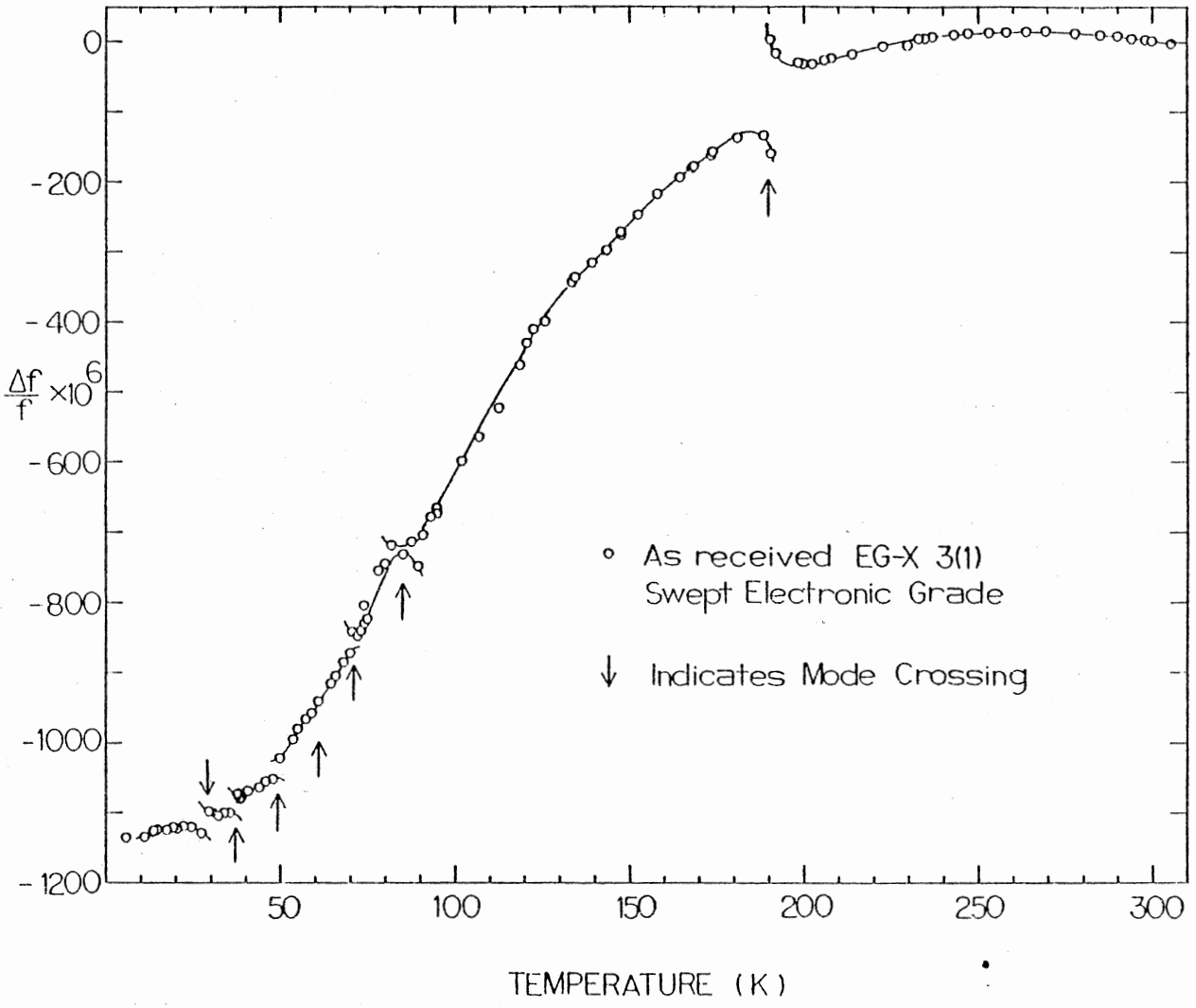

Figure 12. The Normalized Frequency-Temperature Plot for As Received Swept Electronic Grade Resonator EG-X 3(1) (where $f/f \quad (f_T - f_{300})/f_{300}$)

Above 50 K, the acoustic loss decreases steadily until it reaches a minimum at about 90 K. There is a small loss at 54 K which may be due to residual sodium ions not removed by the sweeping process. From a relation developed in Chapter VI, the concentration of the Al-Na^+ defect can be estimated from the size of the acoustic loss at 54 K: The sodium concentration is then $(1.03 - 0.90) \times 10^{-6}$ 1.3×10^{21}, or about 1.7×10^{14} cm^{-3}, which is extremely small by comparison with the Al content (from infrared measurements) of about 2.5×10^{17} cm^{-3}.

The next major features are the small loss peaks at 105 K and 125 K which are superimposed on a slowly increasing background. The 105 K loss peak has been observed by King and Sander (24) who suggest that it is due to the $[Al_{e^+}]^{o}$ centre (a substitutional Al ion, charge compensated by a hole in an adjacent non-bonding oxygen p orbital). This loss peak identification should be regarded as tentative. The 105 K and 125 K loss peaks are probably related as the effect of irradiation on both is similar.

There is a broad loss which extends from about 95 K to 220 K and is centered at 168 K. This has not been identified, although it is probably hydrogen-related. The principal interstitial impurity in the swept Electronic Grade quartz is hydrogen as the alkali ions have been removed by the sweeping process. The technique for evaluating the effectiveness of the sweeping process (i.e., determination of what percentage of alkalis have been removed) has been

developed by Markes and Halliburton (34). There is also a possibility that the sweeping process has created a number of hole centers, though recent work in this laboratory (35) indicates that a significant concentration of holes is produced only when sweeping is carried out in vacuum and at temperatures above the $\alpha-\beta$ phase transition. Holes may be introduced by irradiation, principally at low temperatures (34-37). The argument that most of the loss peaks above 100 K are hydrogen-related is a plausible one, especially when the response to irradiation is considered.

The very large discontinuity in the frequency-temperature curve due to the mode crossing at 190 K is also evident in the acoustic loss results at 190 K. Above 200 K there are three acoustic loss peaks at 202 K, 236 K and 257 K. The small loss peak at 202 K is observed in almost all the resonators studied though its size varies considerably. The loss peaks at 236 K and 257 K are large and change dramatically under irradiation.

Radiation Effects

Resonator EG-X 3(1) was removed from the cryostat and irradiated twice at room temperature with 1.5 MeV electrons for 5 minutes each time. Following each irradiation, it was replaced in the holder and the acoustic loss spectrum from 4 K to 300 K was obtained. The results are presented in Figure 13 along with the curve for the as-received resonator. The principal effects of the two room temperature irrad-

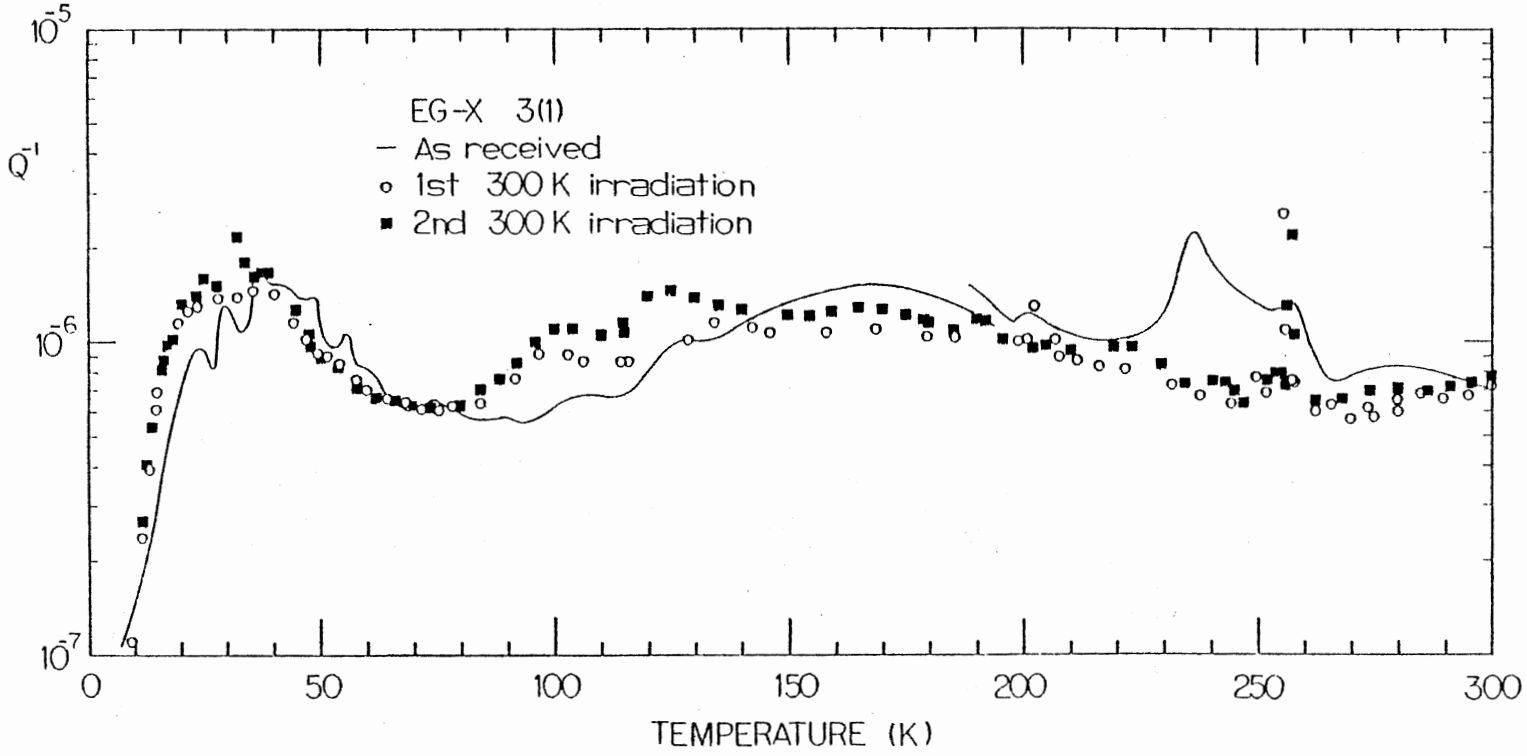

Figure 13. The Acoustic Loss from 4 K - 300 K for Swept Electronic Grade Resonator EG-X 3(1) after Irradiation at Room Temperature

iations are (i) an increase in the 23 K phonon-phonon loss, (ii) a large and dose-dependent increase in the 105 K and 125 K loss peaks, (iii) a reduction in the broad loss centered at 168 K, (iv) complete removal of the 236 K loss peak, and finally (v) a sharp increase in the 257 K loss.

The increase in the 23 K loss peak following irradiation has been observed by Jones and Brown (16), though their interpretation of the loss mechanism was incorrect. The acoustic loss following irradiation is reduced over the temperature range 40 K to 80 K.

Above 80 K, the acoustic loss increases steadily as compared with the as-received value, resulting in a large 105 K loss peak which increases with increasing dose. The 125 K loss peak is also enhanced following irradiation. The very broad loss centered at about 168 K is reduced following the first room temperature irradiation, but appears to be growing back to its initial (unirradiated) value after the second room temperature irradiation. The mode crossing at 190 K does not appear to be affected by the series of irradiations

Apart from the large increase in the 105 K and 125 K loss peaks, the most dramatic effect of the irradiation is the complete removal of the broad 236 K loss peak and the sharp increase in the acoustic loss at 257 K. Above 260 K, the acoustic loss is slightly lower following irradiation, increasing slowly to equal that of the as-received resonator at 300 K.

Discussion

The effects of irradiation on swept and unswept quartz are better understood today as a result of parallel infrared and ESR studies (8, 34-37). The results of these studies will now be described and applied to the interpretation of the acoustic loss data. In the simplest model, the principal defect in high quality synthetic quartz is thought to be aluminum substituting for silicon at a regular lattice site. This substitutional impurity then has one of three charge compensators associated with it, either an alkali ion (Na^+, Li^+), a proton (H^+), or a hole. These centers can be monitered by acoustic loss, infrared, and ESR techniques, respectivly. To date the alkali-compensated Al site has only been directly observed by means of acoustic loss measurements. The Al-Na^+ center gives rise to a peak at 54 K in the acoustic loss. A small acoustic loss peak at 105 K has been associated with the Al-Li^+ center by Fraser (7, 17), however, this interpretation should be regarded as suspect in view of the acoustic loss data presented in this chapter and in chapter VII. There is no known infrared absorption associated with either the Al-Na^+ or Al-Li^+ centers and, since neither is paramagnetic, they do not give rise to an ESR signal.

The proton-compensated substitutional Al defect is referred to as the Al-OH^- center because the proton is associated with a non-bonding p orbital on an adjacent oxygen. This center does give rise to an infrared absorption because of an OH-stretching mode. Two bands are observed at

3367 cm^{-1} and 3306 cm^{-1}. This center does not give rise to an ESR signal. However, irradiation at 77 K will convert the Al-OH^- center to an Al-hole center. The irradiation generates electron-hole pairs within the material. The $[Al_e+]^o$ center is formed from an Al-OH^- center. The proton acts as the electron trap and is ejected as a hydrogen atom. Both the hydrogen atom and $[Al_e+]^o$ center are paramagnetic and give rise to characteristic ESR absorption signals. The hole compensated aluminium center does not appear to give rise to any infrared absorption bands. Neither the Al-OH^- nor $[Al_e+]^o$ centers have been conclusively associated with specific loss peaks in acoustic loss measurements on quartz resonators.

In high quality unswept synthetic quartz which has not been irradiated, the majority of the substitutional Al sites will be compensated by alkali ions, principally sodium. The remainder will be compensated by protons. An infrared scan (at 77 K) of as-received unswept quartz will show either a very small or no absorption at 3367 cm^{-1} and 3306 cm^{-1}. Following an irradiation at room temperature, the two bands grow significantly because the alkali ions which had been acting as charge compensators became mobile and were replaced by hydrogen ions at the Al sites. Radiation induced holes will also compete with the hydrogen for the Al sites. Thus, under irradiation at temperatures above 200 K the Al-alkali centers are converted to the Al-OH^- and Al-hole centers. The presence of two infrared bands, instead of one, for the

Al-OH center indicates at least two possible sites at which the hydrogen can reside. A second irradiation at 77 K (and measurement of the infrared absorption without warming above 125 K) completely removes the 3367 cm^{-1} and 3306 cm^{-1} $Al\text{-}OH^-$ bands. These bands are restored if the sample is warmed to room temperature. The low temperature irradiation has converted all the $Al\text{-}OH^-$ to $[Al_e+]^o$ centers, which then thermally decay (due to recombination with hydrogen atoms) as the sample is warmed above 125 K.

Swept synthetic quartz exhibits very different behaviour, allowing it to be rapidly distinguished from unswept quartz. If the sweeping procedure was completely effective then all the alkali ions have been removed from the material and replaced by hydrogen ions. As-received swept quartz exhibits a large infrared absorption at 3367 cm^{-1} and 3306 cm^{-1}. Irradiation of swept quartz at room temperature converts about 10-20% of these $Al\text{-}OH^-$ centers to $[Al_e+]^o$ centers resulting in a corresponding decrease in the infrared absorption bands. The fraction converted will depend on the number of electron traps and the amount of excess hydrogen within the lattice. These hole centers, formed by irradiation, are stable at room temperature if there are no other species present to recombine with them.

Partially-swept synthetic quartz, from which all alkali ions have not been removed will contain a mixture of $Al\text{-}OH^-$ and Al-alkali centers. Irradiation of partially-swept quartz at room temperature will convert the Al-alkali to $Al\text{-}OH^-$ and

$[Al_e^+]^o$ centers and result in an increse in their concentrations. The change in the Al-OH^- (monitored by infrared) and $[Al_e^+]^o$ (monitored by ESR) center concentrations following a sequence of irradiations at 77 K, 300 K, and 77 K allow the alkali, hydrogen, and aluminum concentrations to be determined, and form the basis for a method to evaluate the completeness of the sweeping process (34).

The identification of the 105 K, 125 K, and 236 K, 257 K loss peak pairs on the basis of the effects of room temperature irradiation is not unambiguous. If the quartz from which resonator EG-X 3(1) was fabricated was completely swept to remove all the alkalis, then the as-received resonator should contain principally Al-OH^- centers. About 10-15% of these will be converted to $[Al_e^+]^o$ centers upon room temperature irradiation. There will be no hole centers present in the as-received swept resonator. It is tempting to associate the 105 K and 125 K acoustic loss peaks with the $[Al_e^+]^o$ center, and the 236 K and 257 K loss peaks with the Al-OH^- center in the light of the results of King and Sander (22-24). They showed an increase in the 105 K loss in swept quartz following irradiation at 77 K and attributed it to the AL-OH^- center. However, the 105 K (and 125 K) loss peaks are present in the as-received resonator, and it is now known definitely from the ESR study of Markes and Halliburton that conventional sweeping (below the phase transition temperature) does not induce hole centers in quartz.

The most likely explanation of the acoustic loss data is

that the resonator was not completely swept and so some alkali ions (most likely lithium) were still present at Al sites. Following the room temperature irradiations, the vast majority of these residual alkali centers would be converted to Al-OH^- centers. On the basis of these results, the 105 K and 125 K loss peaks are tentatively identified with the Al-OH^- center. The identification of these loss peaks is discussed further in Chapter VII. The identity of the 236 K and 257 K loss peaks is still unclear. It would be tempting to link the 236 K loss peak with the Al-Li^+ center as it is completely removed following the first room temperature irradiation. A small loss peak at 105 K in the lithium-swept natural quartz resonator was attributed by Fraser (17) to the Al-Li^+ center, but on the basis of the present work this is questionable. Some early experiments on the acoustic loss of lithium-swept Premium Q resonators proved inconclusive in identifying the loss peak due to the lithium center. The correct identification of the lithium acoustic peak, and a knowledge of its behaviour under irradiation is very important because it is known that lithium-doped synthetic quartz exhibits good tolerance to radiation (1, 21).

CHAPTER V

RADIATION-INDUCED MOBILITY OF SODIUM IONS IN QUARTZ

Introduction

In this chapter the effects of irradiation at various temperatures on the Al-Na^+ defect are examined by means of the acoustic loss technique (38). Since the Al-Na^+ center is the major point defect in as-grown synthetic quartz, understanding its behaviour under irradiation is crucial to the development of radiation hardened quartz. The results of parallel infrared (8) and ESR (34) studies are also presented in this chapter. The results of all three techniques are shown to correlate extremely well and overall give a very good understanding of the interaction of radiation with the Al-Na^+ defect.

The study of the effects of radiation on quartz began with King (14). He found that the large 54 K acoustic loss peak in natural and synthetic 5 MHz AT-cut quartz resonators was completely removed following irradiation at room temperature. This resulted in a large positive offset in the resonant frequency. A similiar result was obtained by Jones and Brown (16). This loss peak occuring at 54 K was later shown by Fraser (17) to arise due to the

presence of sodium. As a result, early synthetic quartz resonators which invariably contained large amounts of sodium did not make very radiation resistant oscillators. Later it was found that synthetic quartz which had been swept to remove the sodium was more radiation resistant. Thus, the key to understanding radiation resistance in quartz comes from an understanding of the mobility of sodium and the other interstitial charge compensators under ionizing radiation.

The recent infrared studies of Sibley et al. (8) and ESR studies of Markes and Halliburton (34) have examined the effects of irradiation on swept and unswept synthetic quartz. Irradiation of unswept quartz at temperatures above 200 K was found to produce infrared bands at 3367 cm^{-1} and 3306 cm^{-1}. These bands are attributed to an unperturbed center formed from a substitutional Al ion charge compensated by a proton which is associated with a non-bonding p orbital on an adjacent oxygen. This $Al\text{-}OH^{-}$ center, which is also produced by sweeping, is thought to be formed by replacing an interstitial alkali ion by a proton at a substitutional Al site.

The ESR results show that following an initial 77 K irradiation of unswept quartz a small number of $[Al_{e^+}]^{o}$ (hole) centers are formed. If the unswept quartz is then irradiated above 200 K and finally at 77 K once more, an enhanced concentration of the unperturbed hole center is observed compared to that produced by the first low temp-

erature irradiation. The initial low temperature irradiation of unswept quartz produces few $[Al_e+]^o$ centers because the Al-alkali defect is stable at 77 K. The few hole centers that are produced are probably formed from Al-OH^- centers. During irradiation above 200 K the Al-alkali center is unstable and the alkali ion is replaced by a proton to form the Al-OH^- center. This Al-OH^- center is then readily broken down to form the $[Al_e+]^o$ center by the second irradiation at 77 K.

The infrared and ESR results indicate that the hydrogen in the Al-OH^- center is mobile under irradiation at any temperature (above 7 K) whereas an interstitial sodium ion (and possibly lithium also) only becomes mobile when irradiated at temperatures above 200 K. The one serious drawback of both studies was that in each case the mobility of the alkali ions (presumed to be sodium) was being measured indirectly. The infrared measurements only yielded the Al-OH^- center concentrations as there are no known Al-Na^+, Al-Li^+, or $[Al_e+]^o$ infrared absorption bands. Similarily the ESR measurements only monitored the $[Al_e+]^o$ center as there is no direct evidence for the presence of Al-alkali centers in the ESR spectrum. The acoustic loss technique, on the other hand, enables a direct measurement of the concentration of the Al-Na^+ centers through the height of the 54 K loss peak and, thus, can unambiguously tell when the sodium ion moves from the substitutional aluminum.

Irradiation and Annealing Studies

An acoustic loss study of the mobility of sodium ions in quartz as a function of the irradiation temperature was initiated. A Premium Q resonator, D1445 DC(2), which had been swept with sodium to enhance the 54 K loss peak was initially examined. The acoustic loss spectrum from 4 K to 100 K for the as-received resonator was obtained and is shown in Figure 14. The resonator was then irradiated with 1.5 MEV electrons for 2 minutes at 77 K and the acoustic loss remeasured. The 54 K loss peak was unaffected by this 77 K irradiation. Following irradiation at 215 K, the sodium loss peak was reduced, and it was completely removed following the 300 K irradiation.

The results from this resonator show that the sodium ion at an Al^{3-} site does indeed become mobile under irradiation at a temperature of around 215 K. The resonator was mounted in the angled holder for horizontal irradiation, but was not damped. This led to the high Q's observed below 10 K. The two loss peaks at 35 K and 42 K are due to interfering modes and they are removed by the 300 K irradiation. This is not surprising as the sodium ions which were at the Al sites have now been dispersed through the lattice changing its mechanical properties.

Following this experiment it was decided to determine more precisely the temperature range in which the sodium ion first becomes mobile under irradiation. Accordingly, an unswept Electronic Grade resonator, EG-S 7(1), which

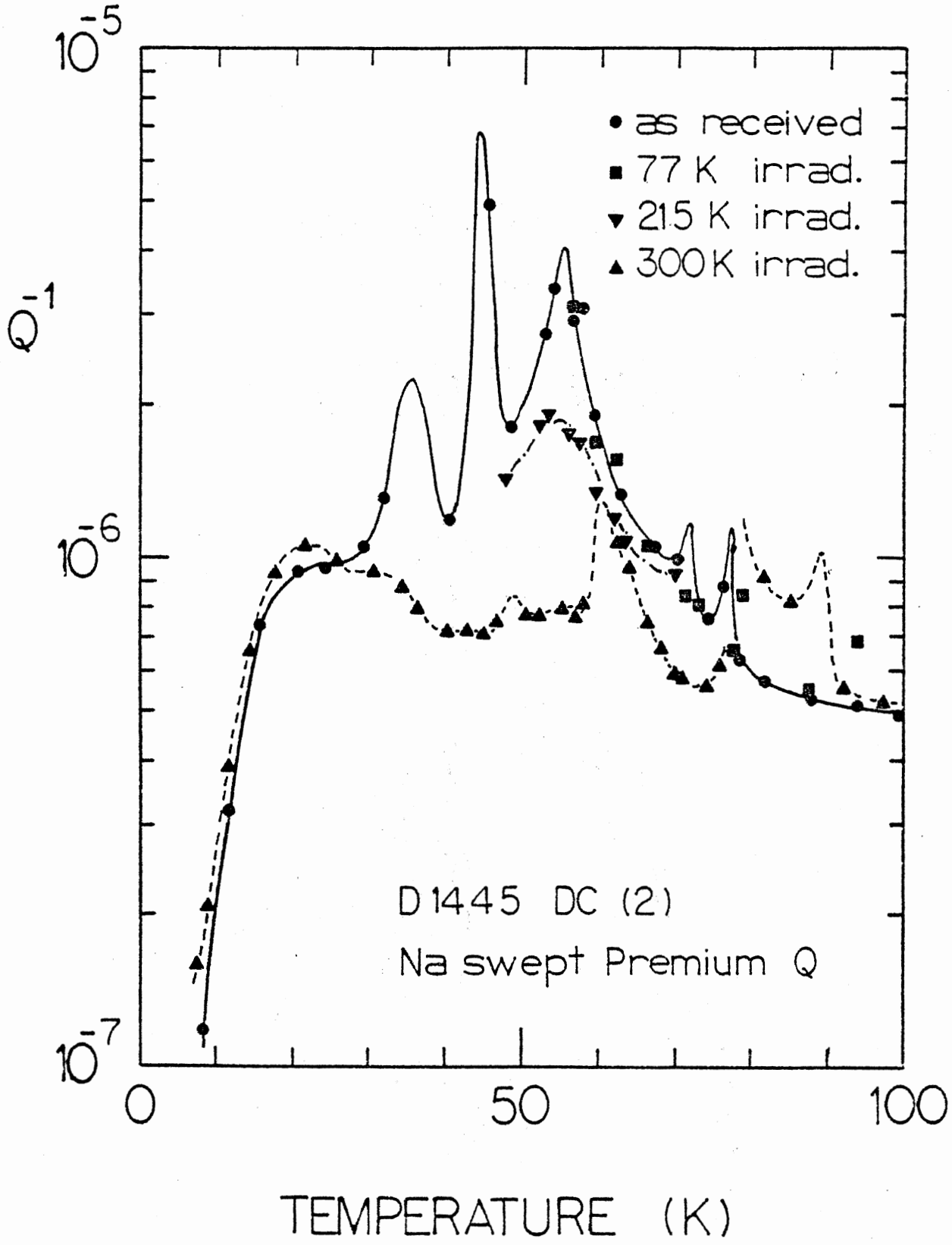

Figure 14. The Acoustic Loss from 4 K - 100 K for Sodium Swept Premium Q Resonator D1445 DC(2) As Received and following Irradiation at 77 K, 215 K, and 300 K

contained more sodium than the resonator D1554 DC(2), was examined. The acoustic loss spectrum was obtained from 4 K to 100 K for the resonator in the as-received state and following irradiation at 180 K, 200 K, 220 K and 250 K. The acoustic loss was measured at the 5th and 7th overtones (5 MHz and 7 MHz, respectively). The results show no change following irradiation at 180 K and a slight reduction in the sodium loss peak after irradiation at 200 K. Figures 15 and 16 show the acoustic loss in the as-received state and following irradiation at 220 K (when the sodium loss peak was reduced by about 20% of its initial value) for the 5th and 7th overtones respectively. The temperature at which the greatest loss occurs is shifted to higher temperatures for the higher frequency overtone. This was the only resonator for which the acoustic loss of overtones other than the 5th were measured. All other acoustic loss measurements refer exclusively to the 5th overtone.

The acoustic loss spectrum of resonator EG-S 7(1) was measured from 4 K to 300 K following the irradiation at 250 K during which the sodium loss peak was completely removed. The resonator was then removed from the cryostat and annealed at 748 K for 10 minutes. This anneal procedure has been shown to remove all radiation damage centers observed by infrared and ESR spectroscopy in unswept material. The acoustic loss was measured again from 4 K to 300 K and the two results are shown together in Figure 17. The annealing procedure has completely restored the sodium

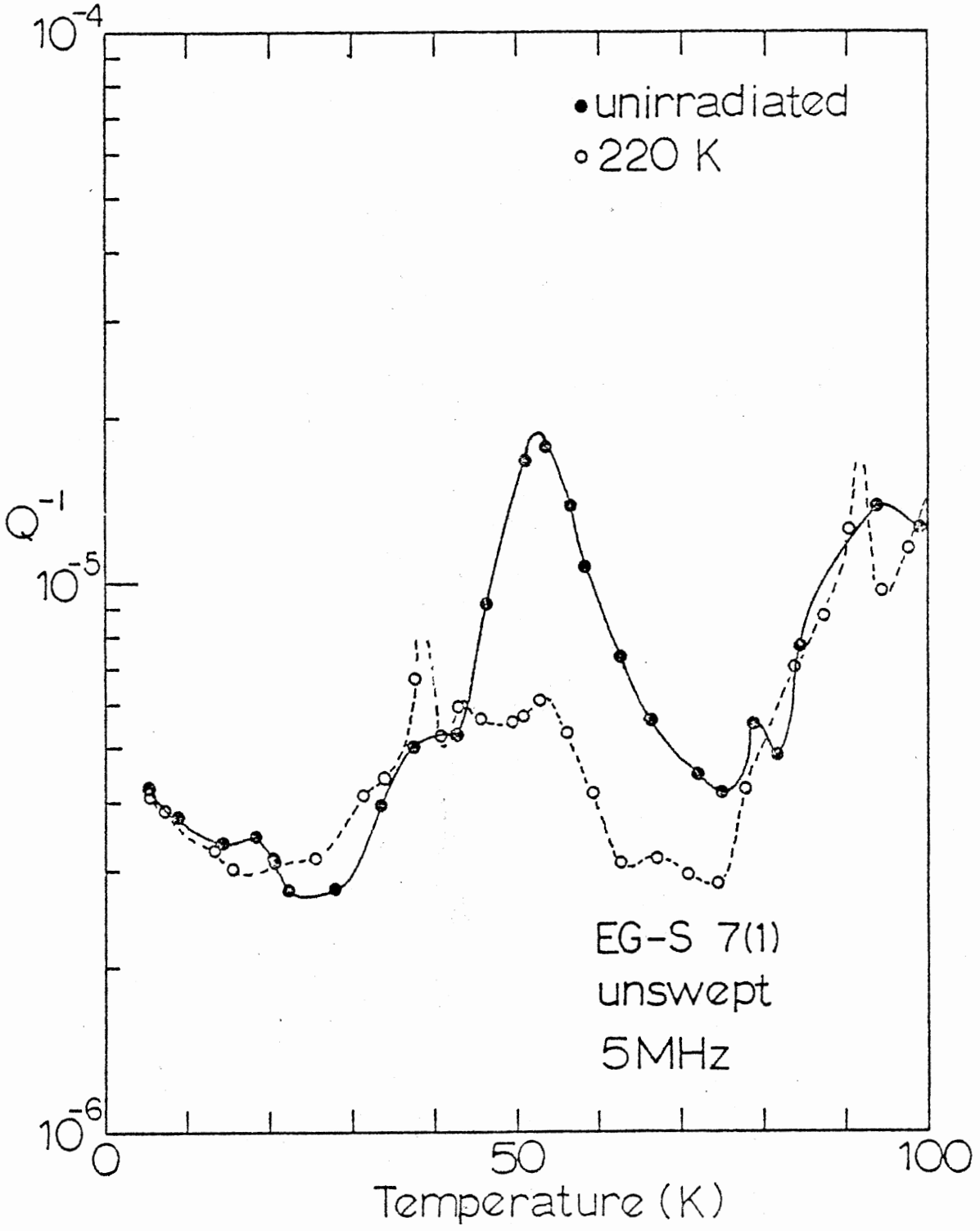

Figure 15. The Acoustic Loss at 5 MHz from 4 K - 100 K for Unswept Electronic Grade Resonator EG-S 7(1) As Received and following Irradiation at 220 K

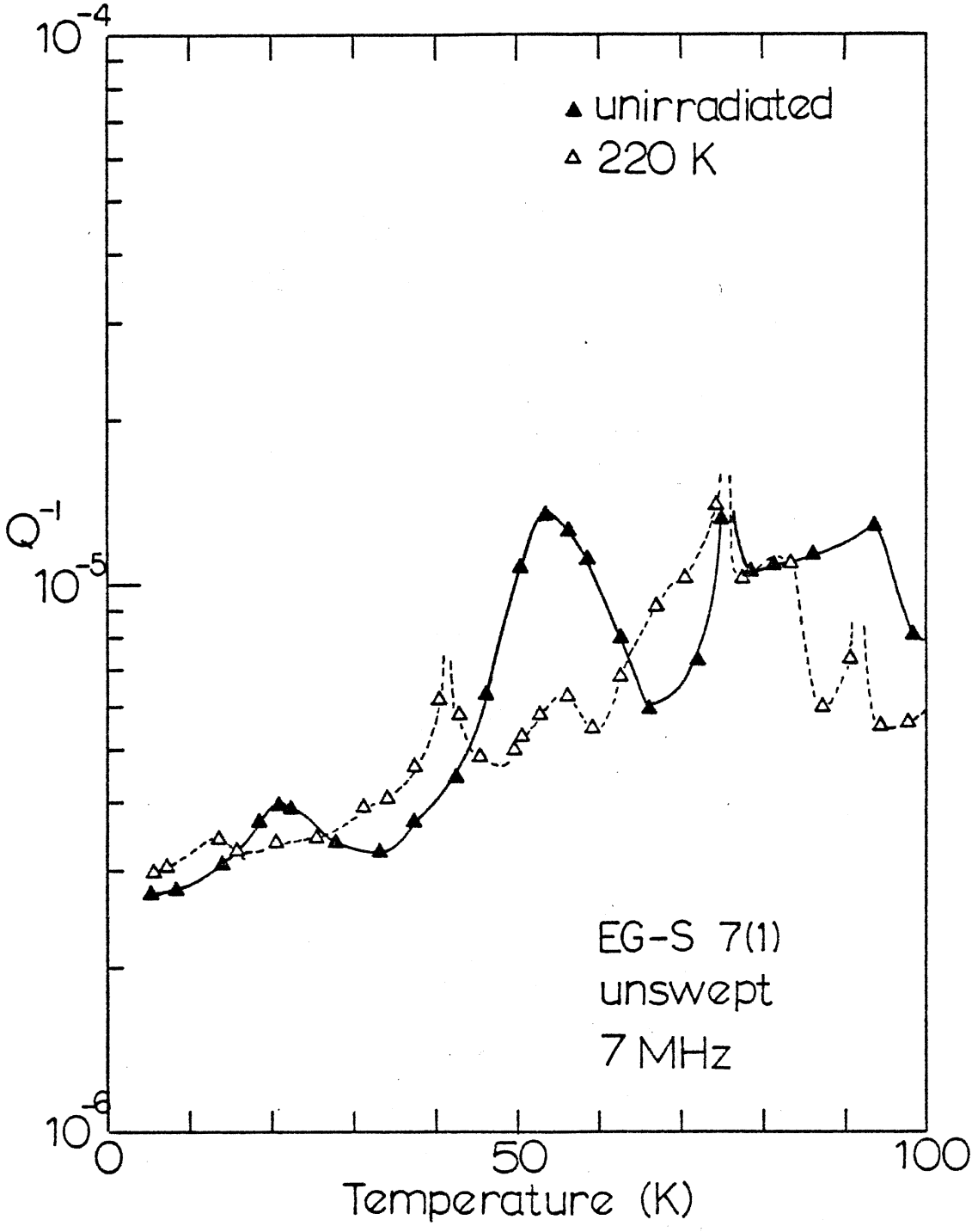

Figure 16. The Acoustic Loss at 7 MHz from 4 K - 100 K for Unswept Electronic Grade Resonator EG-S 7(1) As Received and following Irradiation at 220 K

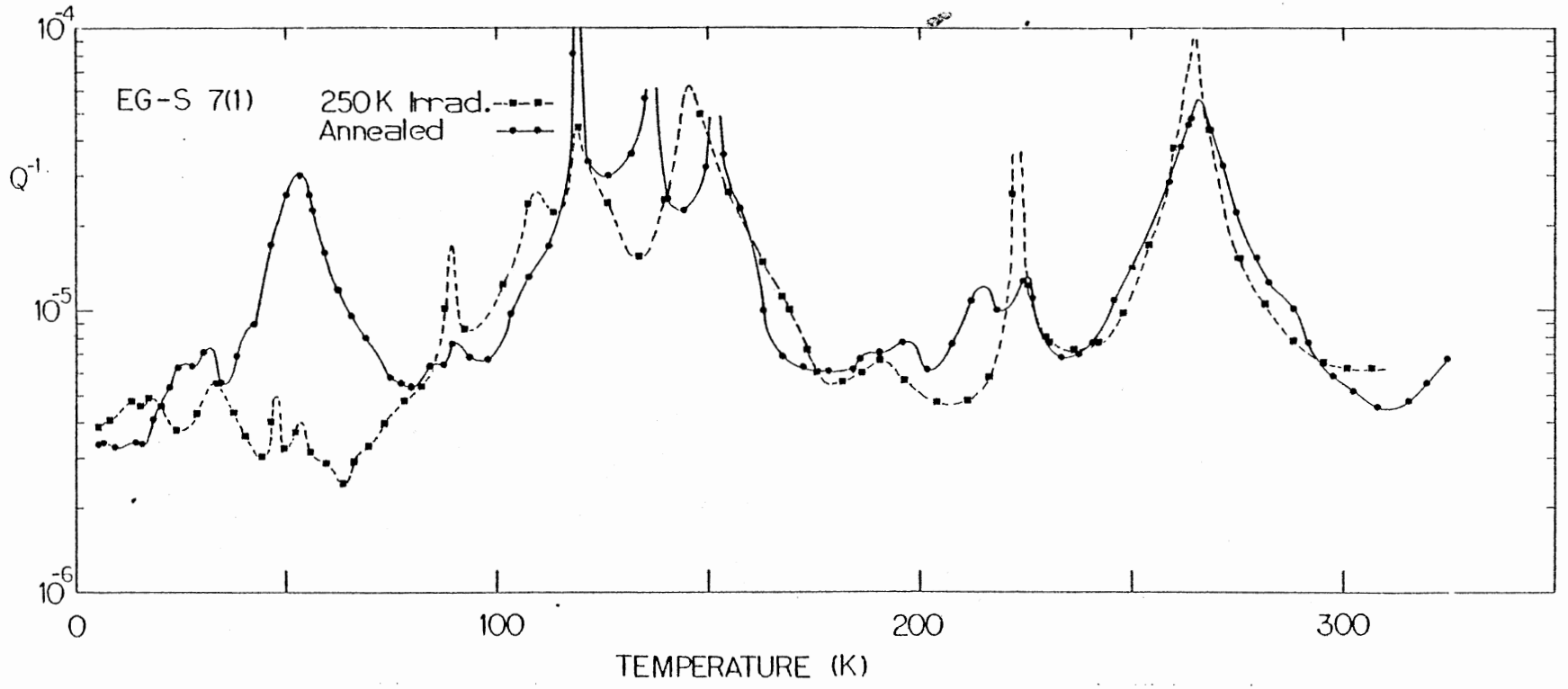

Figure 17. The Acoustic Loss at 5 MHz from 4 K - 300 K for Unswept Electronic Grade Resonator EG-S 7(1) after Irradiation at 250 K and following Annealing at 748 K

loss peak to its origional height. In addition, it has caused changes in the acoustic loss in the temperature range 100 K to 150 K. The origin of the acoustic loss peaks in this region is not conclusively known though they have been observed by Capone et al. (21) who attributed them to coupled modes. There are also a number of other distinct loss peaks above 200 K which will be the subject of discussion in Chapters VII and VIII.

Discussion

The overall results of the acoustic loss, infrared, and ESR studies are shown in Figure 18. The acoustic loss measurements from D1445 DC(2) and EG-S 7(1) have been combined and are presented in the form of the fractional change in the height of the 54 K acoustic loss peak as a function of the irradiation temperature. This Figure illustrates clearly the onset of the irradiation-induced mobility of the sodium at temperatures above 200 K and the consequent reduction in the Al-Na^+ center concentration. The infrared results show the corresponding increase in the Al-OH^- center concentration. The ESR results (following an extra 77 K irradiation which converts Al-OH^- into $[Al_e^+]^o$ (hole) centers) show a similar growth in the hole concentration over the same temperature range.

The acoustic loss results combined with the infrared studies of Sibley et al. (8) and the ESR studies of Markes and Halliburton (34) suggest the following model for the

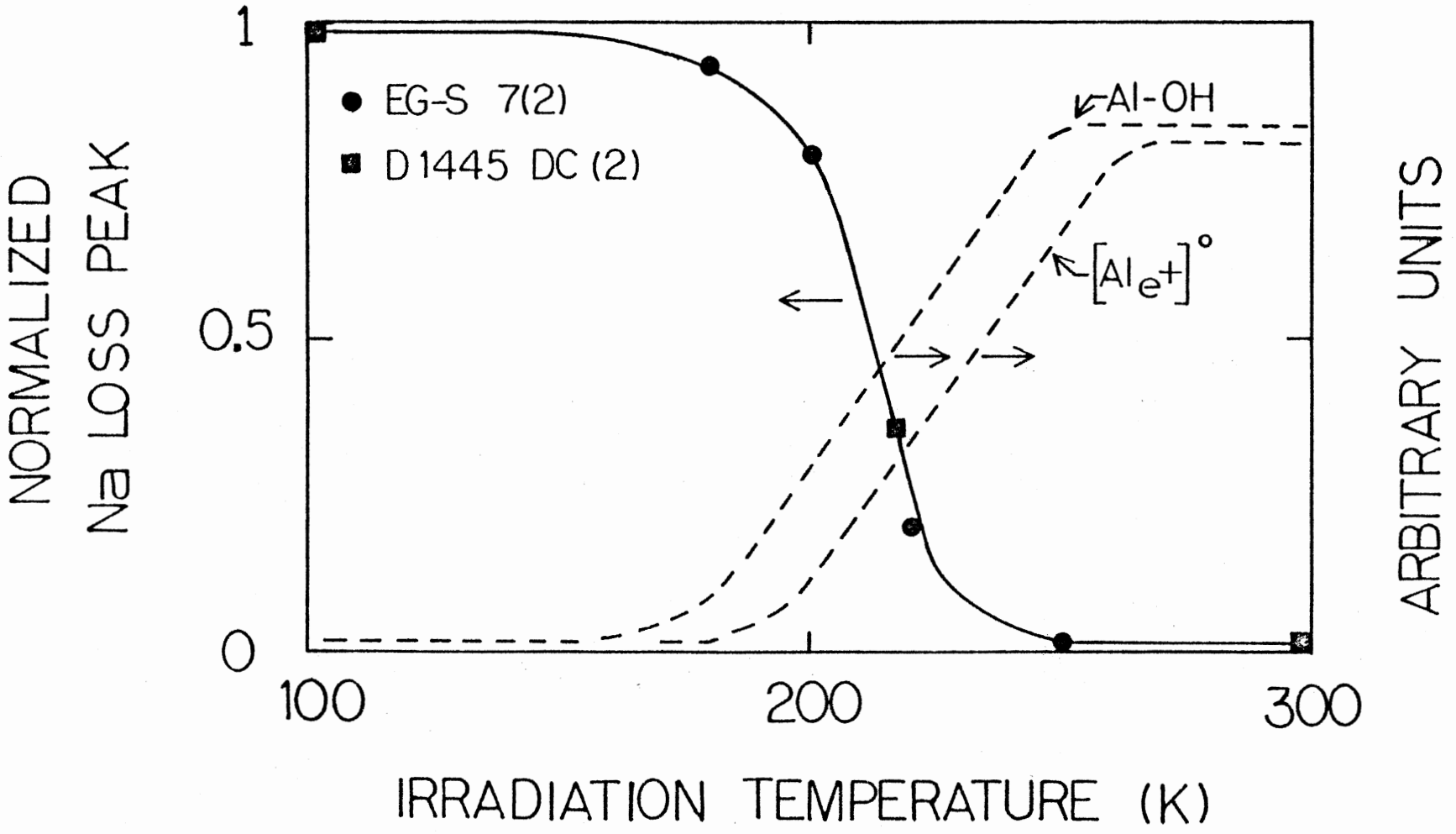

Figure 18. The Change in the Normalized Sodium Loss, Q^{-1}/Q_o^{-1}, along with the Al-OH^- and Al_e^- ^{o} Center Concentrations as a Function of Irradiation Temperature

radiation response of the center formed by a substitutional Al^{3+} ion and an interstitial Na^{+} charge compensator. In as-received unswept quartz, the major point defect is the $Al\text{-}Na^{+}$ center and the $Al\text{-}OH^{-}$ center is not present in observable quantities. The $Al\text{-}OH^{-}$ center is produced from the $Al\text{-}Na^{+}$ center by irradiation if the sample temperature is above 200 K. The interstitial sodium ion becomes mobile under irradiation at these temperatures and moves away from the Al site. Subsequently, a hydrogen ion is trapped on an adjacent oxygen to form the $Al\text{-}OH^{-}$ center. Depending on the number of electron traps available, some Al sites will trap holes to form $[Al_e^{+}]^{o}$ centers rather than $Al\text{-}OH^{-}$ centers (34-37). Since hydrogen is mobile under irradiation at all temperatures, a subsequent low temperature irradiation will convert the $Al\text{-}OH^{-}$ centers to $[Al_e^{+}]^{o}$ centers. An initial low temperature irradiation does not affect the $Al\text{-}Na^{+}$ centers so the initial concentration of $[Al_e^{+}]^{o}$ centers is small.

CHAPTER VI

DIRECT ELECTRODIFFUSION OF QUARTZ RESONATOR BLANKS

Introduction

In this chapter the direct sweeping of quartz resonator blanks is examined. The results of sweeping sodium into a previously unswept Electronic Grade resonator, EG-S 7(2), are presented. This resonator was fabricated from the same bar of quartz (and at the same time) as the resonator used in the previous chapter (EG-S 7(1)). The results of subsequently sweeping sodium out of this resonator are also shown, along with the associated changes in the frequency-temperature curves. The complete removal of sodium from the bulk resonator by the second sweeping is demonstrated.

The use of the sweeping technique, pioneered by King (14), has proved extremely valuable in the identification of acoustic loss peaks in quartz resonators (7,17). However a principal difficulty associated with sweeping is the long time lag between the initial sweeping of the lumbered bar and the final acoustic loss measurements on the fabricated resonator. Current industrial estimates are that the turnaround time is of the order of a year, with a

cost per resonator of approximately $1000 (39).

The role of the direct sweeping of resonator blanks at Oklahoma State University is to permit more rapid identification of specific acoustic loss peaks in quartz rather than to produce precision radiation-hardened resonators. Indentification of the loss peaks and knowledge of their interaction with radiation promise the development of systematic screening procedures which in conjunction with the sweeping technique will assure a constant supply of radiation-hardened quartz.

Results and Discussion

Sodium was swept into resonator blank EG-S 7(2) using the apparatus described in Chapter III. The resonator was ultrasonically cleaned, rinsed with distilled water, and oven dried before sweeping. NaCl (in a supersaturated solution) was deposited on the flat side of the plano-convex resonator. The resonator was then mounted in the graphite holder with a platinum foil between the flat NaCl coated side and the positive electrode. The electrolysis was carried out in vacuum with an applied voltage of 450 V for 24 hours. This voltage gave an electric field of about 2100 V/cm across the resonator. The same procedure with the NaCl coating and platinum foil omitted was used to sweep the sodium out of the resonator.

A room temperature irradiation of an optical sample cut from bar EG-S followed by an infrared scan at 77 K

indicated that the bar contained approximately 1 x 10^{17} cm^{-3} Al-OH^- centers after the irradiation (8). If the sodium sweeping was completely effective, then the resonator should have 1 x 10^{17} Al-Na^- centers. A list of the resonators used and their defect concentrations is given in Appendix A.

The acoustic loss spectrum for EG-S 7(2) from 4 K - 100 K after sodium was swept into the resonator is shown in Figure 19. The loss peak at 54 K is clearly due to sodium as the height of the peak (less the background) is 70 x 10^{-6} after sodium had been swept into the resonator. By comparison, the acoustic loss at 54 K for EG-S 7(1) in the as-received state was 14 x 10^{-6} (Figure 15). This implies a five fold increase in the sodium concentration after EG-S 7(2) was sodium-swept if a linear correlation is assumed between the magnitude of the 54 K acoustic loss and the Al-Na^+ center. Following the second sweeping to remove sodium from the resonator, the 54 K loss peak (less the background) was reduced to 1.5 x 10^{-6} .

A third sweeping run to once more put sodium back into the crystal was unsuccessful as the resonator failed to oscillate when placed in a test holder and excited. It is probably only feasible to sweep resonators a maximum of two or at very most three times. Other workers have observed failure in devices fabricated from quartz which have been swept more than twice (29).

A relation has been developed between the Al-Na^+ center concentration and the acoustic loss maximum at 54 K.

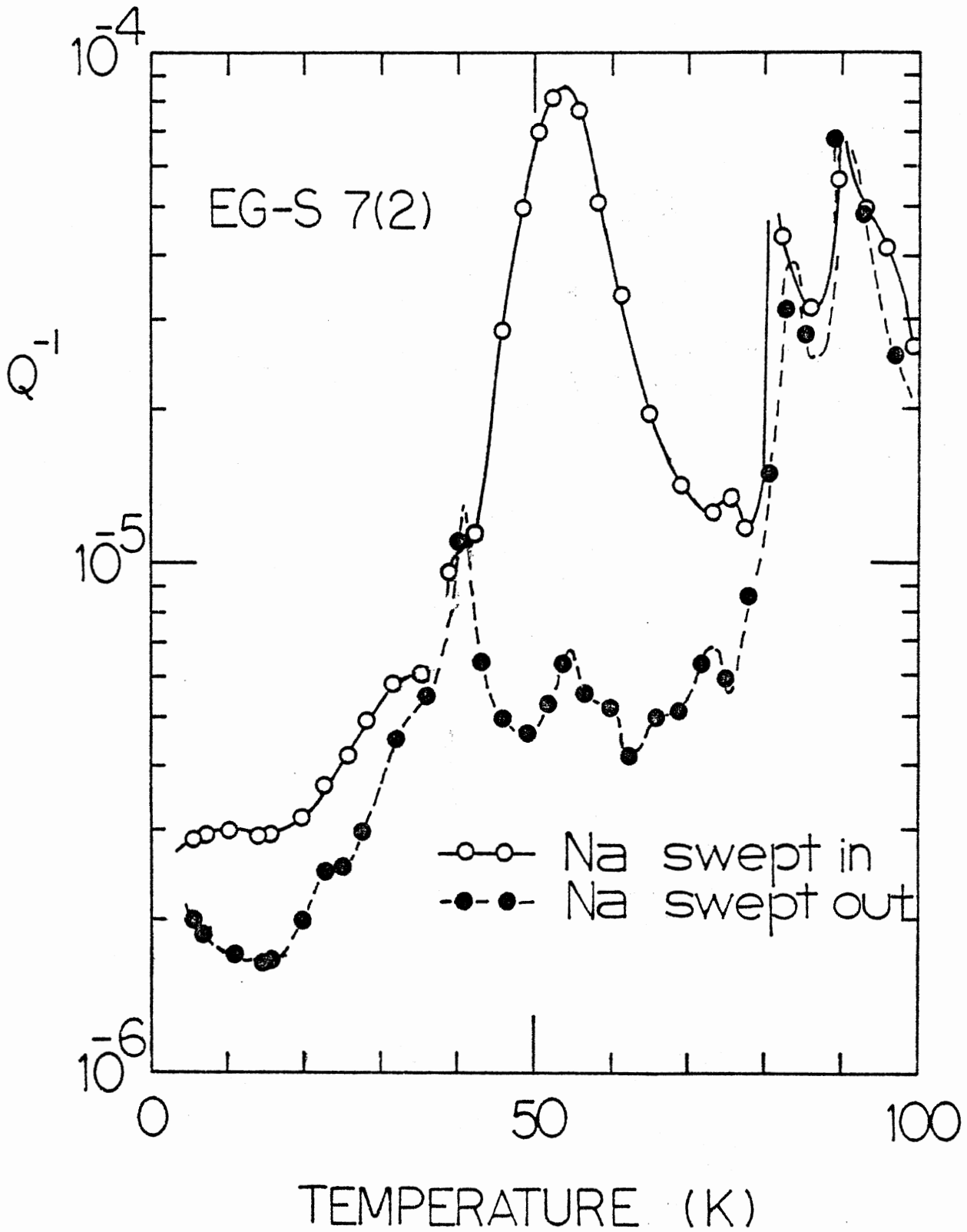

Figure 19. The Acoustic Loss for Electronic Grade Resonator EG-S 7(2) after Sodium was Swept In, and Swept Out

Assuming total conversion upon sweeping, the number of Al-Na^+ centers is taken to be equal to the number of Al-OH^- centers as measured by infrared methods prior to sweeping. The relation can be written as

$$n = A \Delta Q^{-1} \tag{1}$$

where n is the defect concentration (cm^{-3}) and ΔQ^{-1} is the height of the acoustic loss maximum (less the background). For EG-S 7(2),

$$A = \frac{9.6 \times 10^{16}}{7.1 \times 10^{-5}} = 1.35 \times 10^{21}. \tag{2}$$

This expression is used to estimate the Al-Na^- concentration of a number of resonators in the Appendix.

The effect of the removal of the 54 K loss peak (by sweeping in this case) on the frequency of the resonator is shown in Figure 20. The positive frequency offset following the removal of the acoustic loss peak is

$$\frac{\Delta f}{f} = Q_{max}^{-1} . \tag{3}$$

Thus, the expected change in the normalized frequency at temperatures above the sodium loss are of the order of the loss itself, 7.1×10^{-5} or 71 ppm. The measured frequency shift is 80 ppm. Thus if this resonator blank were packed up and used in a precision oscillator circuit, irradiation at room temperature would cause a positive offset in the output frequency of 70-80 ppm.

The changes in the acoustic loss below the operating temperature of the resonator are responsible for the

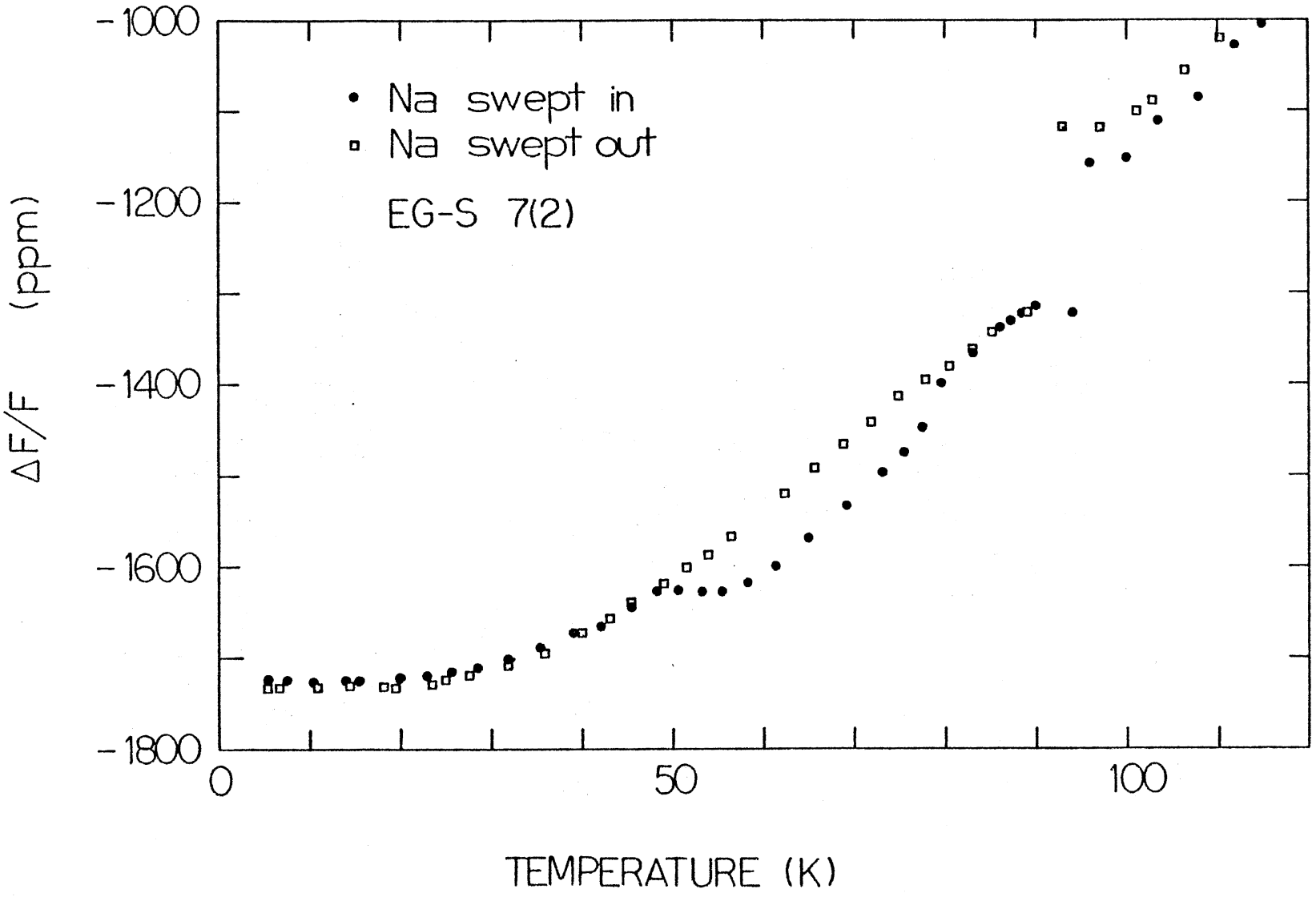

Figure 20. The Normalized Frequency Plot for EG-S 7(2) after Sodium was Swept In and Out

frequency offsets observed during and after irradiation. No study of the transient or steady state effects of radiation on the resonant frequency of a quartz resonator is complete if the changes in the acoustic loss below the operating temperature are not considered. The acoustic loss peaks reflect the fundamental defect centers present within the resonator which, in turn, directly affect the resonant frequency at the operating temperature. The identification of the defect centers which affect the acoustic loss and a knowledge of their interaction with radiation is crucial to the development of radiation-hardened quartz.

A final experiment was undertaken in this series, which was designed to examine the effects of sweeping AT-cut quartz resonators directly. It was suggested that perhaps the sweeping process was not actually removing the sodium ions from the resonator, but merely rearranging them within the lattice in the same way that radiation did. To examine this hypothesis, the resonator EG-S 7(2) (after the sodium had been swept out) was etched in HF briefly (to remove any Na ions on the surface) and then annealed at 748 K for 10 minutes. Annealing above 450^{o}C is known to restore the 54 K loss peak to the as-received value in resonators which have been previously irradiated above 200 K (Chapter V). Following the thermal anneal, the acoustic loss spectrum was measures from 4 K to 100 K. This is shown in Figure 21. The major effect of the annealing was an increase in the overall baseline which is consistent with earlier observations

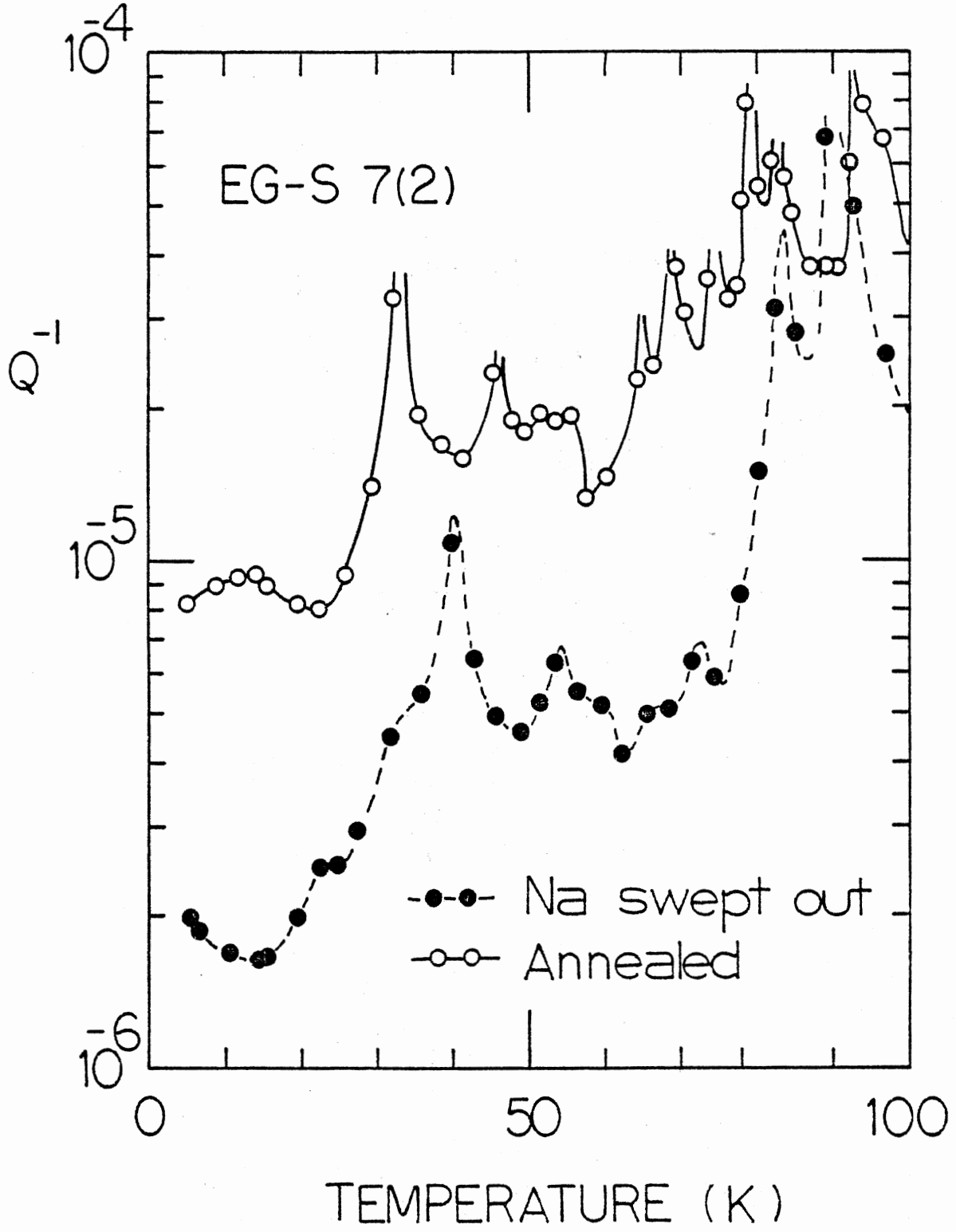

Figure 21. The Acoustic Loss from 4 K - 100 K for Electronic Grade Resonator EG-S 7(2) after Sodium was Swept Out, and following Annealing at 748 K

(Chapter V, Figure 17).There is no noticeable 54 K loss peak after the anneal, demonstrating beyond all doubt the removal of the sodium ions from the resonator by the sweeping process.

The results of this series of experiments have shown that it is quite feasible to sweep 5 MHz 5th overtone AT-cut quartz resonator blanks directly. In addition, annealing studies have demonstrated the completeness of the sweeping process in removing sodium from the resonator. This series of experiments confirms beyond all doubt the identity of the 54 K acoustic loss peak and opens up the possibility of performing other defect identification studies much more rapidly than is currently possible.

CHAPTER VII

DEUTERATION OF QUARTZ RESONATOR BLANKS

Introduction

This chapter is concerned with quartz resonator blanks which have been swept in a hydrogen, and deuterium atmosphere, making use of the techniques developed in the last chapter. This series of experiments involved saturating the number of hydrogen-related acoustic loss peaks, and then replacing the hydrogen with deuterium ($^2H_1$). The Al-OH^- and Al-OD^- center concentrations were monitored by means of infrared absorption. Following the sweeping studies, the resonators were irradiated at 77 K and the acoustic loss was measured from 77 K to 145 K. The resonators were then cooled to 77 K, and the acoustic loss was remeasured. Three resonator blanks were studied, PQ-B 1(4), EG-X 3(2), and PQ-BL 1. The principal results are (i)the association of the 105 K loss with the Al-OH^- center, (ii)the tentative association of the 236 K acoustic loss peak with the Al-Li^+ center, and (iii)the tentative association of the 100 K loss peak with the $[Al_e+]^o$ center.

An unswept Premium Q resonator, PQ-B 1(4), was first studied. The acoustic loss from 4 K - 330 K was measured for the as-received resonator, and following sweeping in a

hydrogen, and then a deuterium atmosphere (Figure 22). The overall results from this resonator are not encouraging. The most striking feature is the very large acoustic loss at 200 K which is only slightly affected by the two sweeping runs. There is a small amount of sodium present as shown by the size of the 54 K acoustic loss. Two loss peaks at 105 K and 117 K grow in following the hydrogen sweep. The loss peak at 105 K is removed following the deuterium sweep.

Two further resonators were studied, PQ-BL 1, a swept Premium Q resonator (fabricated by the Bliley Corporation (40) and supplied by Dr. A.F. Armington (29)) and EG-X 3(2), a swept Electronic Grade resonator similiar to that used in chapter IV. The Bliley resonator was by far the best resonator examined throughout the present study. It had an average Q of approximatly 2.5 million from 80 K - 350 K, as shown in Figure 23. There are a number of interfering modes, but no major loss peaks present. The infrared spectrum showed no measurable Al-OH^- absorption bands in this resonator, implying a very low Al content (less than 1xx 10^{16} cm^{-3}). Because of this, the effects of deuteration on the acoustic loss spectrum are minimal. The resonator was then irradiated at 77 K and the acoustic loss measured immediatly from 77 K - 145 K (Figure 24). The resonator was then cooled to 77 K and the acoustic loss remeasured from 77 K to 145K. Following the 77 K irradiation there are sharp loss peaks at 86 K and 100 K, which disappear following annealing to 145 K.

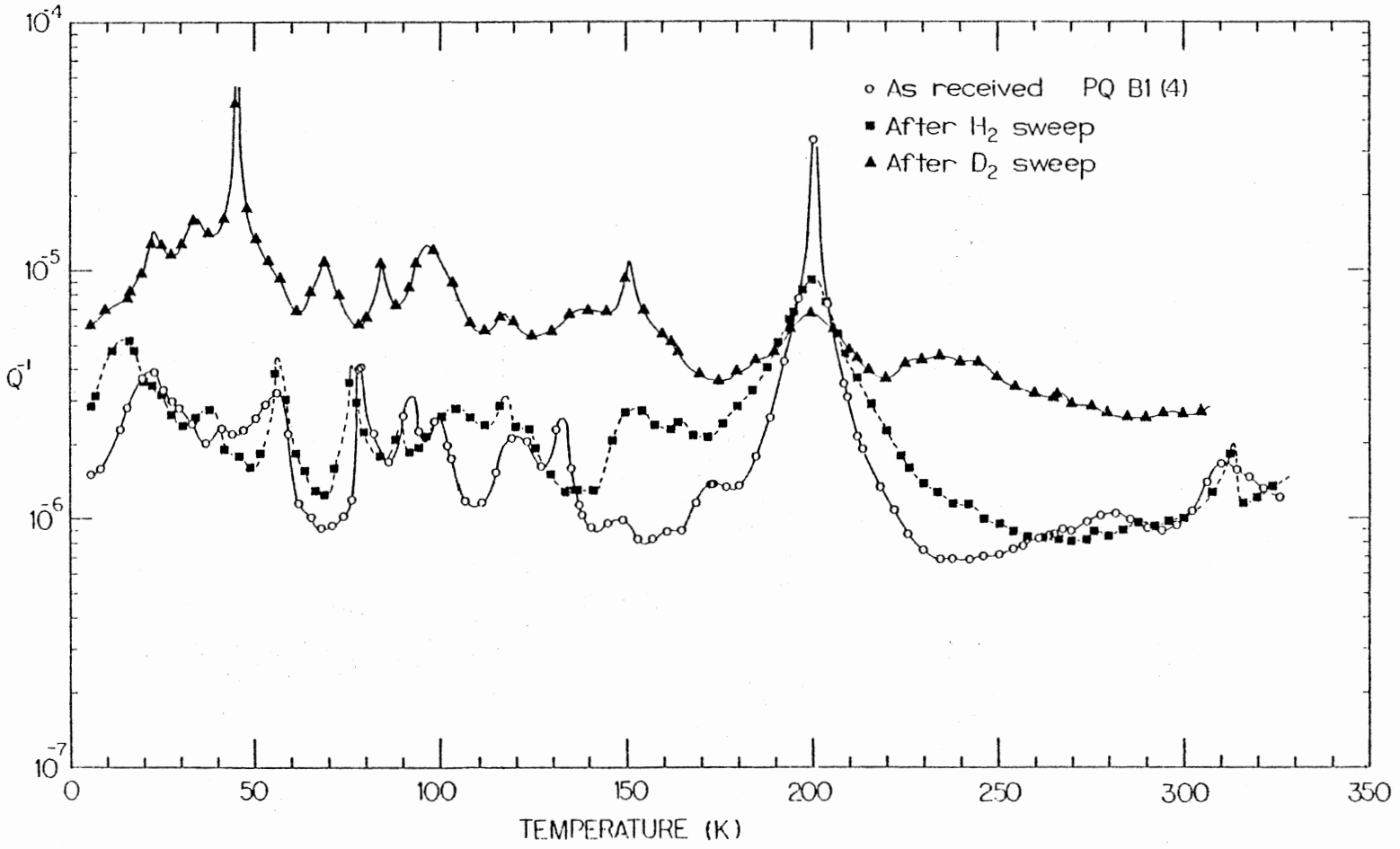

Figure 22. The Acoustic Loss from 4 K - 350 K for Unswept Premium Q Resonator PQ-B 1(4) As Received and following Hydrogen and then Deuterium Sweeping

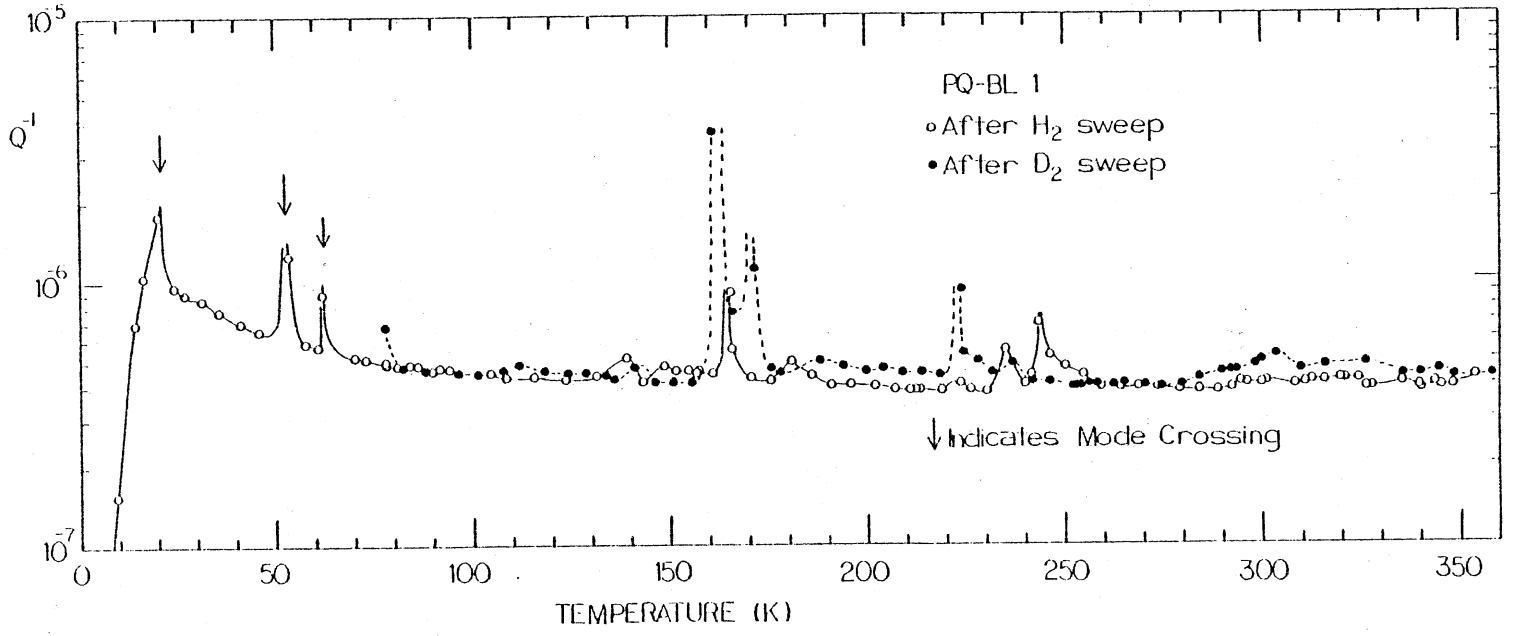

Figure 23. The Acoustic Loss from 4 K - 350 K for Swept Premium Q Resonator PQ-BL 1 following Hydrogen and then Deuterium Sweeping

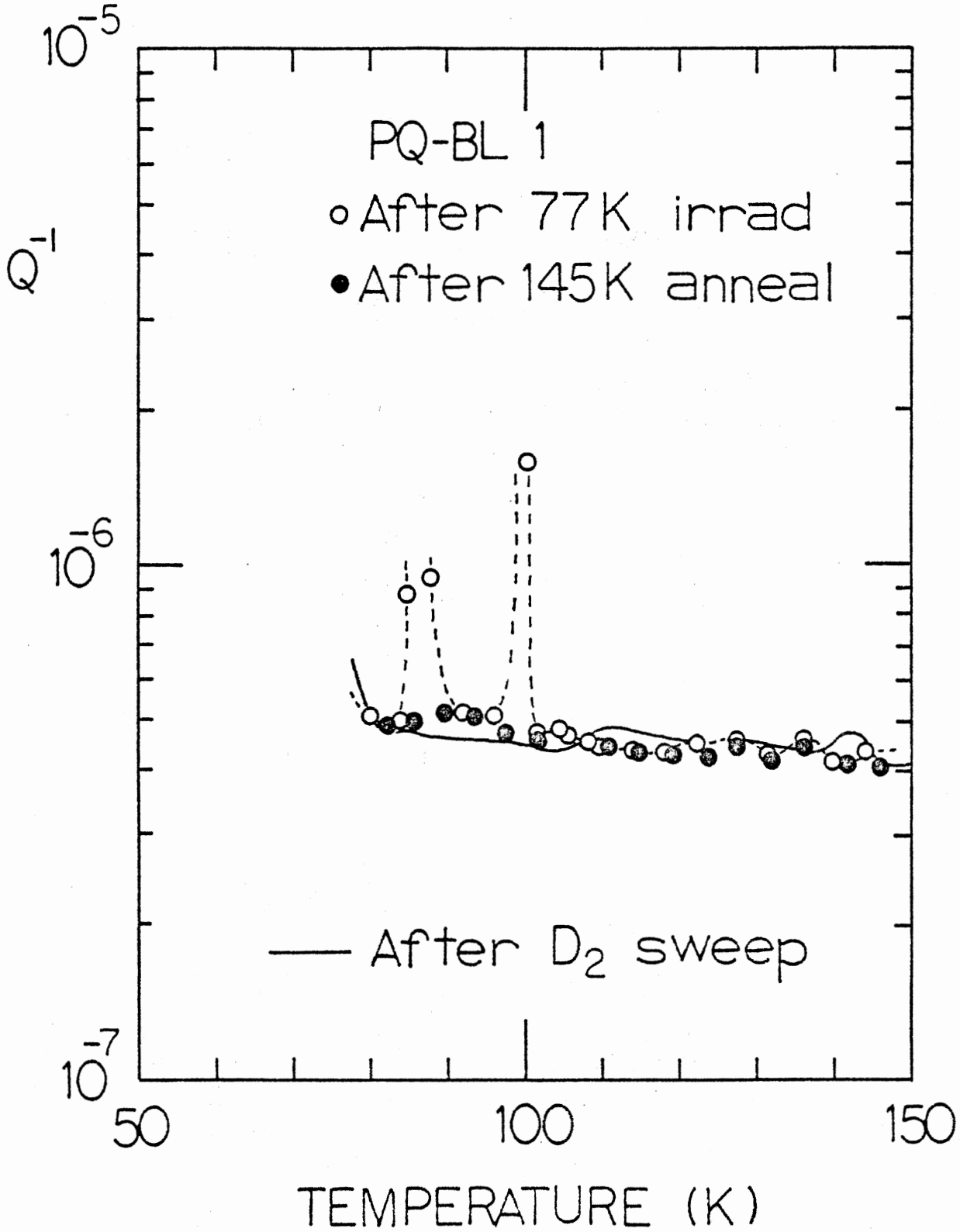

Figure 24. The Acoustic Loss from 77 K - 145 K for Swept Premium Q Resonator PQ-BL 1 following Irradiation at 77 K and Annealing at 145 K

The swept Electronic Grade resonator, EG-X 3(2), was initially swept in a H_2/partial D_2 atmosphere. The acoustic loss spectrum, shown in Figure 25, is very similiar to that for EG-X 3(1) (shown in Figures 11 and 13). There are two differences though, the 105 K loss peak which grows in under irradiation at room temperature in EG-X 3(1) is much larger in the hydrogen swept EG-X 3(2). Following the hydrogen sweep, the Al-OH^- center concentration was 2.4 x 10^{17} cm^{-3}. The resonator was then swept in deuterium three times, monitoring the Al-OH^- and Al-OD^- concentration each time. The final concentrations were 1.1 x 10^{17} cm^{-3} and 1.3 x 10^{17} cm^{-3}, respectivly.

Following deuteration the 105 K loss peak is completely removed and the acoustic loss is lower up to 140 K. There is a small loss peak at 140 K superimposed on the rising baseline. The loss peak at 252 K is slightly reduced in width, but otherwise unaffected. Irradiation at 77 K induces a sharp loss peak at 100 K which disappears on annealing to 145 K (Figure 26). The acoustic loss is then higher from 100 K - 150 K following the irradiation and subsequent annealing.

Discussion

The loss peak that occurs at 105 K is particularly interesting because it is present in a number of resonators examined in this study. It has also been observed by King (14) and Fraser (17). King observed two loss peaks, at 100 K

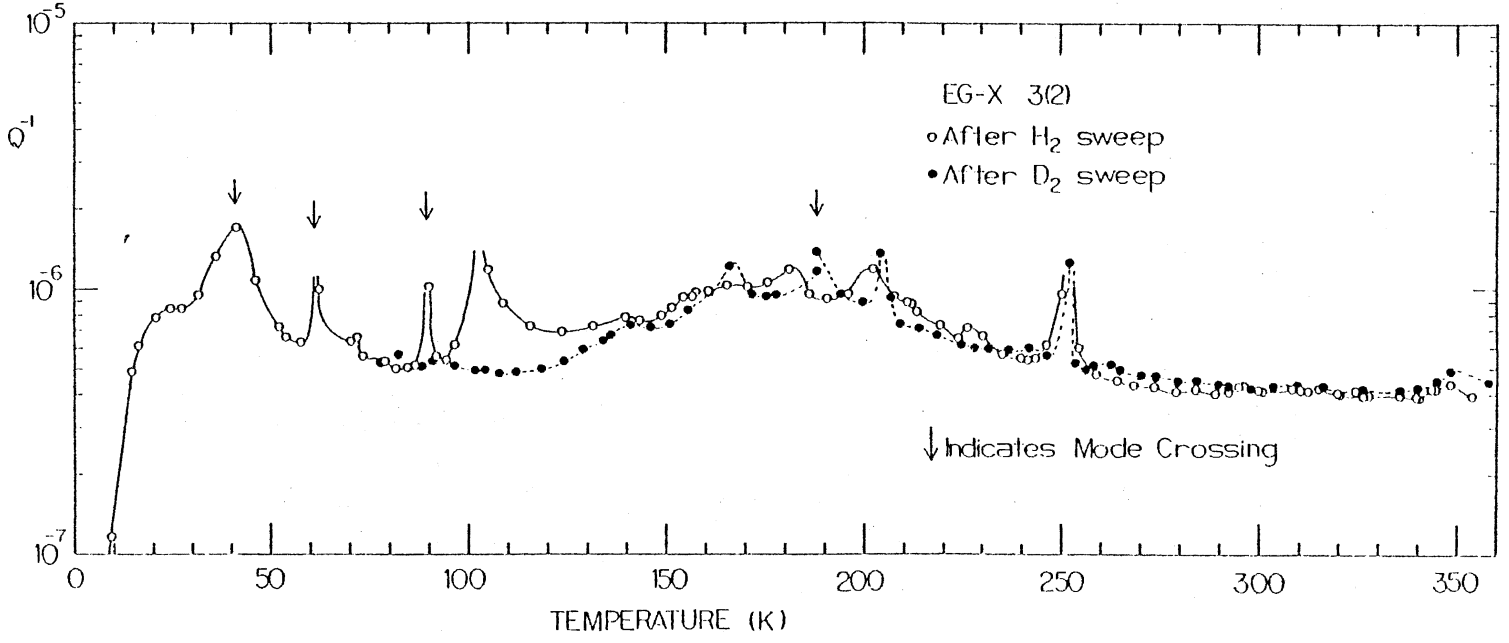

Figure 25. The Acoustic Loss from 4 K - 350 K for Swept Electronic Grade Resonator EG-X 3(2) following Hydrogen and then Deuterium Sweeping

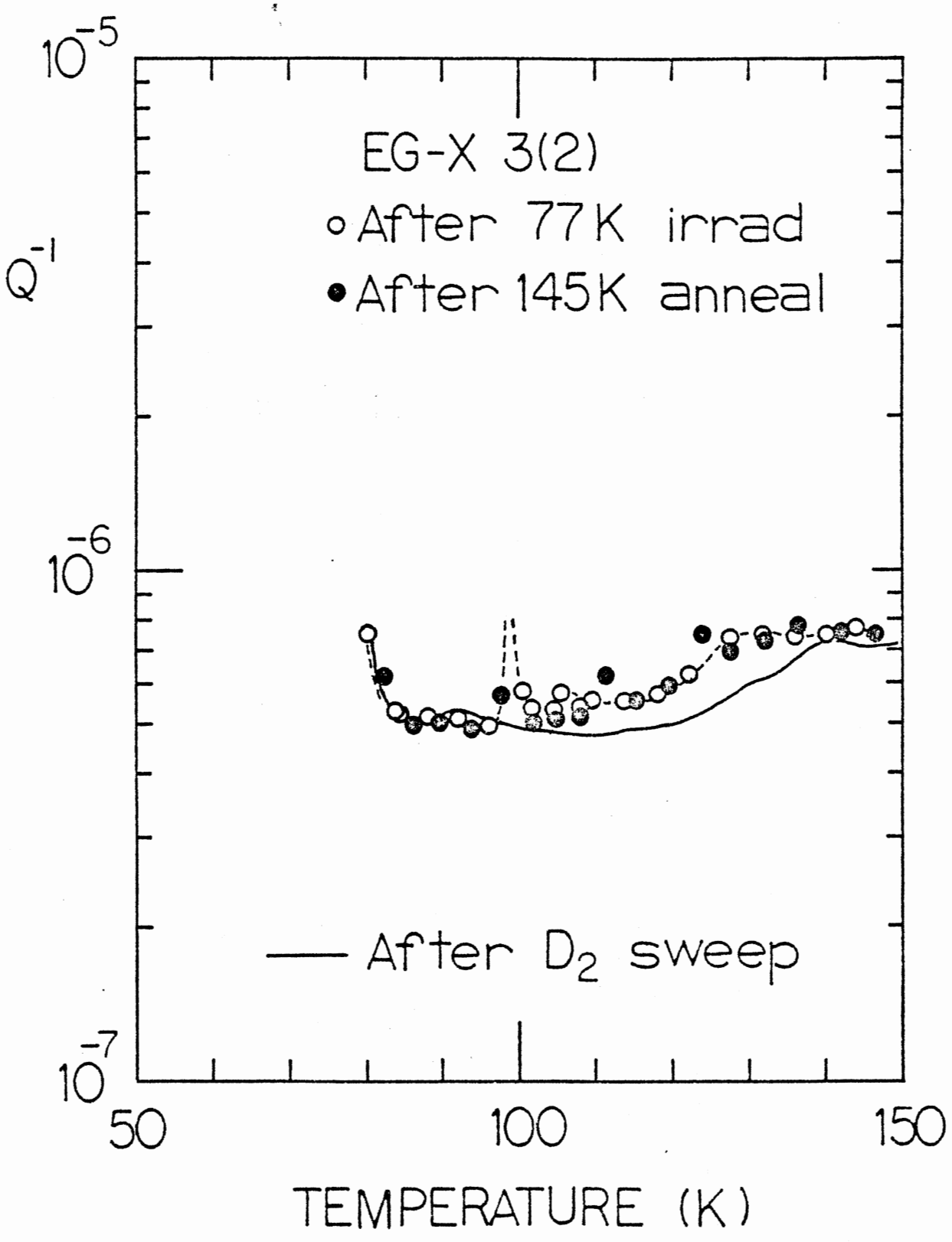

Figure 26. The Acoustic Loss from 77 K - 145 K for Swept Electronic Grade Resonator EG-X 3(2) following Irradiation at 77 K and Annealing at 145 K

and 105 K, in both natural and early synthetic quartz, following irradiation at room temperature. Fraser attributed a small loss peak at 105 K in lithium-swept natural quartz to the Al-Li^+ center. King and Sander (22) reported a loss peak at around 100 K following irradiation of swept natural quartz at 77 K. They also observed a loss peak at 115 K which annealed out when the temperature was raised above 165 K. The 100 K loss peak was attributed to the $[Al_{e^+}]^o$ center.

The as-received sodium-swept Premium Q resonator, D1445 DC(2), which was used in the study of the radiation-induced mobility of sodium, also exhibits a loss peak at 105 K (Figure 27). After the 300 K irradiation, a large loss peak at 123 K grew in.

The unswept Electronic Grade resonator, EG-S 7(1), also used in that study, shows a loss peak at 105 K following irradiation at 250 K. This is completly removed following annealing at 748 K for ten minutes (Figure 17).

The swept Electronic Grade resonator, EG-X 3(1), has two small loss peaks at 105 K and 125 K, which grow in following irradiation at 300 K (Figure 13). After sweeping in hydrogen, the swept Electronic Grade resonator, EG-X 3(2), exhibits a large loss at 105 K which is completly removed following deuteration.

All of these observations are consistent with the identification of the 105 K acoustic loss peak with the Al-OH^- center. The acoustic loss results for EG-X 3(1) and

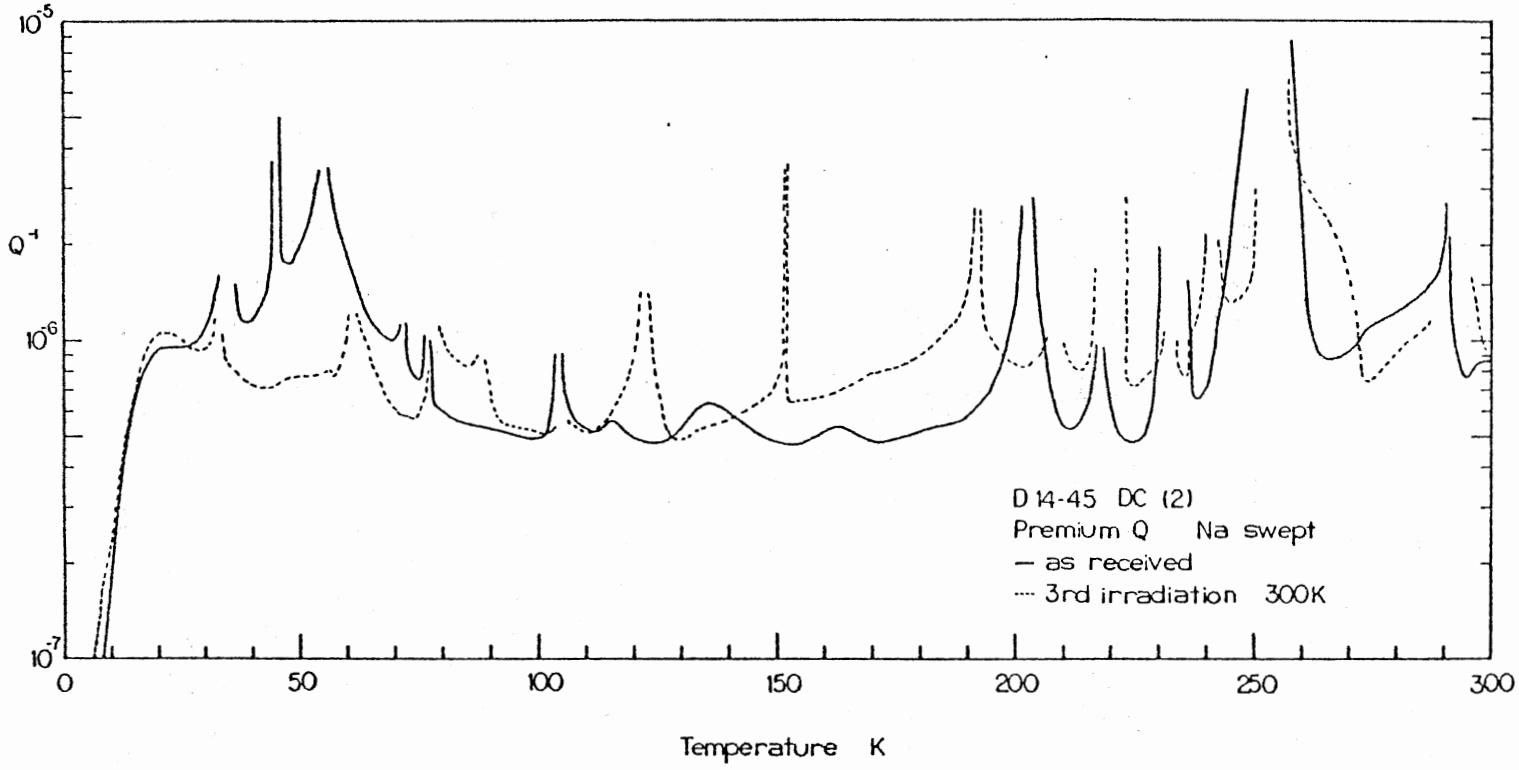

Figure 27. The Acoustic Loss from 4 K - 300 K for Sodium Swept Premium Q Resonator D1445 DC(2) As Received and following Irradiation at 300 K

3(2) imply that these resonators were not completly swept as-received, because the 105 K loss peak grows in following irradiation at room temperature or sweeping in hydrogen. Since the sodium content was small (Chapter IV), the most likely charge compensating ion remaining at the Al sites is lithium. Thus the 236 K loss peak, which is removed in EG-X 3(1) by irradiation at 300 K is tentativly identified with the Al-Li^+ center. This loss peak is absent in the hydrogen swept EG-X 3(2), supporting this identification.

The Premium Q resonator, D1445 DC(2), will have both Al-Na^+ and Al-OH^- centers unless the sodium-sweeping was complete. Upon irradiation at 300 K, all the Al-Na^+ centers are converted into Al-OH^- centers. The 123/125 K loss peak also seems to be associated with the Al-OH^- center, as it grows in with the 105 K acoustic loss. This may be due to a second site at which the proton can reside (c.f. the two Al-OH^- infrared absorption bands at 3367 cm^{-1} and 3306 cm^{-1}) or it may be due to an alkali-perturbed Al-OH^- center. The loss peak at 105 K in EG-S 7(1) after irradiation at 250 K and its subsequent removal following annealing at 748 K is completly explained by associating it with the Al-OH^- center. Following the high temperature anneal, the sodium ions migrate back from their trapping sites and recombine to form Al-Na^+ centers once more, eliminating the Al-OH^- centers.

The association by King and Sander (22) of the 100 K loss peak with the $[Al_{e^+}]^o$ center was examined by

irradiating the deuterated resonators at 77 K and then measuring the acoustic loss immediately from 77 K to 145 K. The acoustic loss spectra for resonators PQ-BL 1 and EG-X 3(2) (Figures 24 and 26) show the growth of a sharp loss peak at 100 K which disappears following annealing at 145 K. This loss peak is narrower and smaller than those observed by King (14) and King and Sander (22). This is probably due to the lower aluminum content in these two resonators. The results of these experiments tends to confirm the association of the 100 K acoustic loss peak with the $[Al_{e^+}]^o$ center.

The observation by King (14) of large 100 K and 105 K acoustic loss peaks in (unswept) natural and early synthetic quartz as a result of irradiation at 300 K can now be fully explained. It is known from parallel ESR studies (34) that irradiation at room temperature of swept and unswept synthetic quartz generates stable hole centers. In swept quartz, the percentage of Al-OH^- centers converted to $[Al_{e^+}]^o$ centers can vary from 10% - 25%. The actual percentage depends on the number of electron traps avaliable and is higher in unswept quartz. Irradiation of natural quartz, which contains a higher aluminum and interstitial impurity content, should result in the formation of a large percentage of $[Al_{e^+}]^o$ centers. King's observations are most easily explained by assuming the formation of approximatly equal numbers of $[Al_{e^+}]^o$ and Al-OH^- centers. The smokey coloration observed in natural quartz (and low grade

synthetic quartz) following irradiation has been shown to be related to the $[Al_e+]^o$ center in a parallel study by Koumvakalis (41).

CHAPTER VIII

CONCLUSIONS AND FUTURE RESEARCH

Principal Conclusions

This has been the first systematic study of the radiation-induced mobility of sodium ions in synthetic quartz resonators. The sodium ion compensating a substitutional aluminum ion (the Al-Na^+ defect), was found to become mobile when irradiated at temperatures above 200 K. The sodium concentration as a function of irradiation temperature was monitored by means of the height of the 54 K acoustic loss peak, and correlated extremly well with parallel infrared and ESR studies (8,34,37). A relation was developed between the height of the acoustic loss peak at 54 K and the absolute Al-Na^+ center concentration.

Direct electrodiffusion of quartz resonator blanks was investigated and the results of sweeping sodium into, and out of, an Electronic Grade resonator were obtained. A subsequent annealing study demonstrated the complete removal of the sodium from the bulk crystal. In addition, direct infrared measurements on quartz resonators were pioneered to determine the aluminum content from the Al-OH^- absorption bands at 3367 cm^{-1} and 3306 cm^{-1}.

Following the sucess of the direct sweeping of sodium

into quartz resonator blanks, a series of experiments was undertaken to identify the hydrogen-related acoustic loss peaks by first sweeping the resonators in hydrogen and then in deuterium. The 105 K acoustic loss peak was found to be due to the $Al\text{-}OH^-$ center, and the $Al\text{-}Li^+$ center was proposed as the defect responsible for the 236 K acoustic loss peak. Following a low temperature irradiation of the deuterated resonators, a sharp loss peak was introduced at 100 K. This loss peak, which disappeared after a 145 K anneal, was identified with the $[Al_e+]^o$ center. The development of direct sweeping of quartz resonator blanks promises rapid results in future defect identification studies.

Future Research

The goal of future acoustic loss studies should be to identify and quantify all the loss peaks associated with the $Al\text{-}Na^+$, $Al\text{-}Li^+$, $Al\text{-}OH^-$, and $[Al_e+]^o$ centers. Currently each center must be examined by a different spectrascopic technique. If the $Al\text{-}Na^+$, $Al\text{-}OH^-$, and $[Al_e+]^o$ (and also the $Al\text{-}Li^+$) centers could be followed simultaneously then a much better understanding could be obtained of the 'table of contents', i.e. the relative concentration of defects and impurities in quartz. One drawback is the low sensitivity of the acoustic loss technique (as compared with ESR), but this would be more than made up for by the information gained.

Two sets of experiments are proposed toward an unambig-

uous identification of the acoustic loss peaks due to the Al-OH^- and $[Al_e+]^o$ defects. The first, and shorter set, involves an EG-X or PQ-E resonator which should be swept in hydrogen and the acoustic loss measured from 4 K - 400 K. The resonator should then be cooled to 77 K, irradiated, and immediately cooled to 4 K. The acoustic loss should then be measured from 4 K to 400 K, cooling back to 77 K at the end of each day's measurements (to avoid annealing effects). The results of sweeping in a hydrogen atmosphere should be to introduce a large loss peak at 105 K due to the Al-OH^- center. After irradiation at 77 K, this peak should be significantly reduced or completely removed. At the same time a loss peak should grow in at 100 K due to the conversion of Al-OH^- to $[Al_e+]^o$ centers. Cooling the resonator to 77 K once more, and measuring the acoustic loss from 77 K - 170 K should show the 100 K acoustic loss peak reduced to 10% - 25% of its height following the 77 K irradiation. The 105 K loss peak should be restored to 75% - 90% of its original value. This set of experiments should strongly confirm the proposed identities of the 100 K and 105 K acoustic loss peaks.

A longer series of experiments patterned on the ESR measurements of Markes and Halliburton (34) is also envisaged. These experiments would use resonators fabricated from bar PQ-E, for which extensive ESR and infrared data is avaliable. One of the resonators should

be swept (either in vacuum or preferably in H_2), and the other unswept. The acoustic loss should be measured from 4 K - 350 K for the as-received resonators and then following a series of irradiations at 77 K, 300 K and 77 K.

The as-received swept resonator will contain principally $Al\text{-}OH^-$ centers, with very few $Al\text{-}Li^+$ or $Al\text{-}Na^+$ centers, and no $[Al_e+]^\circ$ centers. The unswept resonator will contain mainly $Al\text{-}Na^+$ and/or $Al\text{-}Li^+$ centers with a few $Al\text{-}OH^-$ centers.

Following the first irradiation at 77 K, the swept resonator (cooled immediately to 4 K) will have all its $Al\text{-}OH^-$ centers converted to $[Al_e+]^\circ$ centers, while the $Al\text{-}Na^+/Al\text{-}Li^+$ centers will be unchanged. The unswept resonator will still have principally $Al\text{-}Na^+/Al\text{-}Li^+$ centers, with the original $Al\text{-}OH^-$ centers becoming a mixture of $Al\text{-}OH^-$ and $[Al_e+]^\circ$ centers.

After the 300 K irradiation, the concentration of $Al\text{-}OH^-$ centers in the swept resonator will have recovered to within 10% - 25% of its original value, with the remainder forming $[Al_e+]^\circ$ centers. All the $Al\text{-}Na^+$ and $Al\text{-}Li^+$ centers will be converted into $Al\text{-}OH^-$ centers. This contribution should be small if the resonator was swept completely. However, in the unswept resonator, all the $Al\text{-}Na^+$ and $Al\text{-}Li^+$ centers will be converted into a mixture of $Al\text{-}OH^-$ and $[Al_e+]^\circ$ centers in a 1:1 ratio.

The second irradiation at 77 K will convert all the $Al\text{-}OH^-$ centers in the swept resonator to $[Al_e+]^\circ$ centers

once more. Thus the acoustic loss peak corresponding to the hole center will increase after this step. In the unswept resonator, all the Al-OH^- will be converted into $[Al_{e^+}]^o$ centers, and so the hole center will also grow in following this irradiation. The concentration of hole centers should be approximatly the same in both resonators after this step.

The reason for undertaking such a long series of measurements is that the behaviour of each of the defects following each step is known. Though there may be differences in the relative sizes of the loss peaks, from step to step, the overall trends of each acoustic loss peak should enable positive identification of the defect associated with it.

The next stage in the acoustic loss measurement program should be to automate the measurement system and to move to transmission techniques to measure the Q and resonant frequency. A device-independent bus system (IEEE-488 1978) is envisaged. An HP 9825S computer/controller is required to sucessfully implement this scheme, along with a new IEEE-488 compatible synthesizer. This system should be implemented in three stages. First, the temperature control system should be automated using the current power supply and digital voltmeter. Second, the new synthesizer and existing timer-counter should be integrated into the computer system while still maintaining the logarithmic decay method. Finally with the purchase

of a bus-compatible digital vector voltmeter, the whole system should be converted over to the transmission technique. An automated acoustic loss measurement system will enable a great many more measurements to be made and at much smaller temperature intervals than is currently feasible. In addition, an automated system, especially with a wide frequency range synthesizer, would allow measurements to be made more easily on a large number of overtone modes. This would enable accurate activation energies to be measured for each acoustic loss peak. Finally, an automated system would also allow for the possibility of transient radiation experiments as well as long term ageing studies.

A final piece of work that needs to be done is the design and construction of a holder for resonator blanks that would allow ESR measurements to be made on them directly. So far in this project, both ESR and infrared measurements have been made on the same samples, and of course both acoustic loss and infrared measurements have been made on resonator blanks. The next step is to make ESR and acoustic loss measurements on the same resonator blank. This would enable an unqualified identification of the acoustic loss peak due to the $[Al_e^+]^o$ center.

Prospects for Radiation-Hardened Quartz

The prospects are excellent for a program to ensure a constant and consistant supply of radiation-hardened quartz

REFERENCES

REFERENCES

(1) Armington, A. F., A. Kahan and F. K. Euler, ETS Technical Memorandum No. 3, Solid State Division, Deputy for Electronic Technology, RADC, Hanscoin AFB, Mass. 01731, September 1976.

(2) Cady, W. G., Piezoelectricity, Vols. I and II (Dover Publications, New York, 1964).

(3) Mason, W. P., Piezoelectric Crystals and their Application to Ultrasonics (D. Van Nostrand, New York, 1950).

(4) Fundamentals of Quartz Oscillators, Application Note 200-2 (Hewlett Packard Inc., 1979).

(5) De Maw, D., Ed. The Radio Amateurs Handbook, 57th Edition (American Radio Relay League, Newington, CT. 06111, 1980).

(6) Crystal Device Measurements Using the Spectrum Analyzer, Application Note AX-3535 (Tektronix Inc., P.O. Box 500, Beaverton, Oregon 97077, 1977).

(7) Fraser, D. B., Physical Acoustics, Vol. 5, W. P. Mason Ed. (Academic Press, New York, 1968), p. 59.

(8) Sibley, W. A., J. J. Martin, M. C. Wintersgill and J. D. Brown, J. App. Phys., 50, 5449 (1979).

(9) Jani, M. G., M.S. Thesis (Oklahoma State University, 1979).

(10) Halliburton, L. E., J. J. Martin and W. A. Sibley (Private Communication).

(11) Warner, A. W., Proc. Inst. Radio Engrs., 40, 1030 (1952).

(12) Bommel, H. E., W. P. Mason and A. W. Warner, Phys. Rev., 99, 1894 (1955).

(13) Bommel, H. E., W. P. Mason and A. W. Warner, Phys. Rev., 102, 64 (1956).

(14) King, J. C., Bell Syst. Tech. J., 38, 573 (1959).

(15) Jones, C. K. and C. S. Brown, Proc. Phys. Soc. (Lond.), 79, 930 (1962).

(16) Jones, C. K. and C. S. Brown, Proc. Phys. Soc. (Lond.), 82, 372 (1963).

(17) Fraser, D. B., J. App. Phys., 35, 2913 (1964).

(18) Mason, W. P. and T. B. Bateman, J. Acoust. Soc. Am., 36, 646 (1964).

(19) Poll, R. A. and S. L. Ridgway, IEEE Trans. Nucl. Sci., NS-13, 130 (1966).

(20) Flanagan, T. M. and T. F. Wrobel, IEEE Trans. Nucl. Sci., NS-16, 130 (1969).

(21) Capone, B. R., A. Kahan, R. N. Brown and J. R. Buckmelter, IEEE Trans. Nucl. Sci., NS-17, 217 (1970).

(22) King, J. C. and H. H. Sander, IEEE Trans. Nucl. Sci., NS-19, 23 (1972).

(23) King, J. C. and H. H. Sander, IEEE Trans. Nucl. Sci., NS-20, 117 (1973).

(24) King, J. C. and H. H. Sander, Radiation Effects, 26, 203 (1975).

(25) Weil, J. A., Proceedings of the 27th Annual Symposium on Frequency control, US Army Electronics Command, Forth Manmouth, N. J., pp. 153-156 (1973). Copies available from the Electronic Industries Assoc., 2001 Eye St., N. W., Washington D. C. 20006.

(26) Berry, B. S. and A. S. Nowick, Physical Acoustics, Vol. 3A, W. P. Mason Ed. (Academic Press, New York, (1966).

(27) Nowick, A. S. and B. S. Berry, Anelastic Relaxation in Crystalline Solids (Academic Press, New York, (1972).

(28) Nowick, A. S., Physical Acoustics, Vol. 13, W. P. Mason and R. N. Thurston Eds. (Academic Press, New York. 1977).

(29) Armington, A. F. (Private Communication).

(30) Kansas Crystal Inc., 1203 Kansas Ave., Kansas City, Kansas 66105.

(31) K-W Manufacturing Co., P.O. Box 508, 919 8th street, Prague, Oklahoma 74864.

(32) Martin, J. J. (Private Communication).

(33) Mason, W. P. and T. B. Bateman, J. Acoust. Soc. Am., 36, 644 (1964).

(34) Markes, M. E. and L. E. Halliburton, J. Appl. Phys., 50, 8172 (1979).

(35) Koumvakalis, N., (Unpublished Studies).

(36) Halliburton, L. E., M. Markes, J. J. Martin, S. P. Doherty, N. Koumvakalis, W. A. Sibley, A. F. Armington and R. N. Brown, IEEE Trans. Nucl. Sci., NS-26, 4851 (1979).

(37) Martin J. J., S. P. Doherty, L. E. Halliburton, M. Markes, N. Koumvakalis, W. A. Sibley, R. N. Brown and A. F. Armington, Proceedings of the 33rd Annual Symposium on Frequency Control, US Army Electronics Command, Fort Monmouth, N. J., pp. 134-147 (1979). Copies available from Electronics Industries Assoc., 2001 Eye St., N. W., Washington D. C. 20006.

(38) Doherty, S. P., J. J. Martin, A. F. Armington and R. N. Brown, J. App. Phys., to be published.

(39) King, J. C., D. Koehler and T. Young (Private Communication).

(40) Bliley Electric Company, 2545 West Grandview Boulevard, P. O. Box 2428, Erie, Pennsylvania 16508.

(41) Koumvakalis, N., J. App. Phys., to be published.

APPENDIX

DEFECT CENTER CONCENTRATIONS FOR RESONATORS EXAMINED IN THIS STUDY

Resonator	Irradiation T (K)	Q^{-1} ($x10^6$) 54 K loss peak	Al^* conc. ($x10^{-16}$ cm^{-3})	Na^* conc. ($x10^{-16}$ cm^{-3})	Na^{**} conc. ($x10^{-16}$ cm^{-3})	Comments
D1445 DC(2)	as rec.	2.7	1.8	0.3	0.36	
	77	2.7				
	215	1.0				
	300	0				
D1445 9b(1)	-	0	0.3	0		
EG-S 7(1)	as rec.	14	9.6		1.9	
	180	13				
	200	11				
	220	2.8				
	250	1				
EG-S 7(2)	-	71	9.6	9.6^{***}	-	Na swept in
	-	1.5	9.6		0.2	Na swept out
PQ-B 1(4)	-	3	1.6		0.4	
EG-X 3(1)	as rec.	0.13	-			
	1st 300		-			
	2nd 300	0	25		1.7×10^{-2}	
EG-X 3(2)	-	0	24			H_2/partial D_2 sweep
	-	0	11			Final D_2 sweep

VITA[2]

Stephen Paul Doherty

Candidate for the Degree of

Doctor of Philosophy

Thesis: RADIATION EFFECTS IN QUARTZ RESONATORS

Major Field: Physics

Biographical:

Personal Data: Born Dublin, Ireland, 28 December 1953.

Education: Received Bachelor of Arts (Natural Science), University of Dublin, Trinity College, May 1975; received Master of Science degree, University of Dublin, Trinity College, April, 1978; completed requirements for the Doctor of Philosophy degree at Oklahoma State University in May 1980.

Professional Experience: National Science Council Fellowship, Summer 1973; teaching assistantship, Department of Physics, Trinity College Dublin, 1974 to 1977; research assistantship, Department of Physics, Oklahoma State University, 1977 to 1980.